The Linear and Nonlinear Biomechanics of the Middle Ear

Thomas Wright

June 2005 Doctoral Thesis Royal Institute of Technology Department of Mechanics SE-100 44 Stockholm,Sweden

TRITA-MEK
Technical Report 2005:11
ISSN 0348-467X
ISRN KTH/MEK/TR- -05/11- -SE

This thesis will be presented at 1000, Wednesday 8th June 2005, room V3, Teknikringen 72, Kungl Teknisksa Högskolan, Valhallagvägan 79, Stockholm.

 \odot Thomas Wright 2005

Abstract

This thesis addresses the biomechanics of the human middle ear, that part of the auditory system which converts sound pressure waves in air to fluid pressure waves in the cochlea. The middle ear's mechanism is analysed in four papers, three main and one supporting; in the main papers the middle ear is treated as a multi-particle, multi-rigid body ensemble possessing a variable number of degrees of freedom depending upon the case being investigated.

It is confirmed, using the standard representation of a single fused incudo-malleal block, that the middle ear's motion is linear, but when this fused block restriction is lifted nonlinearity is present which significantly affects the mechanism's behaviour. In view of the linearity of the chain under the fused block conditions, the explanatory veracity of the conventionally accepted 'fixed axis hypothesis' of ossicular motion is examined and found to be wanting as a realistic description of the chain's physical movement.

The nonlinear behaviour of the ossicular chain centres around the action of the incudo-malleal joint. This joint is shown to have preferential planes of operation, principally the pitch or longitudinal plane and in general to act as an efficient energy dissipator at high driving pressures and low frequencies. Providing the pressure is high enough, it is shown this energy dissipator effect eventually becomes independent of frequency.

The supporting paper discusses the dynamics of the imposition and removal of equation constraints justifying methods used to investigate the functioning of the incudo-malleal joint.

Keywords: biomechanics, middle ear models, ossicular chain.

Acknowledgments

I would like to express my thanks to Professor Martin Lesser for his help and guidance in bringing this work to fruition. The role of thesis advisor is a difficult and complex one and I am grateful to him for his tolerance and forbearing in providing the intellectual freedom to discover for oneself the virtues of focus and simplicity.

I would also like to thank my other colleagues in the Department of Mechanics for their thoughts and conversations on numerous occasions. The department is marked not only by deep erudition in its chosen fields but by a broad span of philosophical, scholarly and humane concerns that leaven the otherwise gritty business of academic production.

Mostly of course I would like to thank Christine. Love is hours spent in helping to photograph hopping mechanical frogs that refuse to hop and being lectured to on the dynamical behaviour of the incudo-malleal joint with no demur, except for an imperceptible glazing over of the eyes.

Contents

1. Ir	ntroduction	1
1	1.1 Scope and aims	1
1	1.2 Outline of thesis	2
1	.3 Statement of authorship	3
2. T	he Middle Ear	4
2	2.1 Anatomy	4
	2.1.1 The tympanic membrane	6
	2.1.2 The middle ear cavities	
	2.1.3 The cochlea	6
2	2.2 The ossicular chain	7
2	2.3 The working of the middle ear and the fixed axis hypothesis	8
2	2.4 Sound measurement	9
	2.4.1 Hearing loss and prosthesis	10
2	2.5 Current research interests	10
3. N .	Iodel constructs and multibody dynamics	12
3	3.1 Conceptual approaches	12
	3.1.1 Electrical analogues and network theory	12
	3.1.2 The classical mechanics of constrained systems	14
	3.1.3 Screw theory	16
3	3.2 Derivation of equations of motion	17
	3.2.1 Underlying approach	18
	3.2.2 Geometry and configuration	19
	3.2.3 Equations of motion	24
	3.2.4 Kineto-static forces and impulses	$\dots 25$

4. Data and computation	27
4.1 Derivation of parameters	27
4.1.1 Geometry and inertial characteristics	27
4.1.2 Material parameters and calculation of applied forces	
4.2 Programing considerations	30
4.2.1 Sophia	31
4.2.2 The solution of equations	
4.3 Numerical model equations	32
4.3.1 2D model	32
4.3.2 Model 1	33
4.3.3 Model 2	35
4.3.4 Model 3	36
5. Conclusions and outlook	40
5.1 Conclusions	40
5.2 Future work	43
5.2.1 Experimental	43
5.2.2 Theoretical	
5.2.3 Prosthesis	46
References	47

Papers

- 1. Modelling of the ossicular chain
- 2. Ossicular vibrations and the fixed axis hypothesis
- 3. The role of nonlinear dynamics of the middle ear $\,$
- 4. The effects of unilateral and bilateral constraint changes in mechanical systems: A paper in support of the study of nonlinear mechanisms in the middle ear

Chapter 1

Introduction

The principal aim of this thesis is to examine the mechanical behaviour of the human middle ear whose function is to transform air borne sound waves gathered by the external ear, into fluid borne pressure waves processed by the inner ear. It seeks to accomplish this task within the conceptual and methodological framework of applied mechanics as manifested by its sub-discipline, multi-rigid body mechanics.

1.1 Scope and aims

All mammals possess middle ear structures interposed between the inner ear (cochlea) and the usually visible outer ear (pinna). Each ear, left and right, has its own middle ear structure and there is considerable structural and geometric similarity in the form of middle ears across the whole of the mammalian species range. This thesis aims to contribute to the understanding of the action of the middle ear by investigating and progressively developing, a number of mathematical models which simulate its dynamical behaviour. To do this the middle ear is viewed as a linked chain of connected bodies, moving in response to externally generated sound waves, transmitting and modifying these waves in such a fashion as to be suitable for the cochlea to process.

Since the science of human hearing involves consideration of a wide range of physical phenomena interacting with physiological, perceptual and psychological factors, the sheer complexity of the subject requires the imposition of suitable simplifying assumptions to aid understanding and facilitate progress. In the pursuit of these needs two major simplifications are inherent in the considerations that follow. Firstly, although hearing is normally a binaural activity, only the singular ear will be considered here thus reducing any binaural interaction to zero. Secondly, although it is recognised that the middle ear is a conveniently defined element operating within a larger system, only modest attention will be afforded to those other elements immediately abutting it, the outer ear and the inner ear. The functioning of these two structures will be accounted for by specifically defined variables which

'flow' into, and out of, the middle ear across its conceptual boundaries.

Bearing these caveats in mind the scope of this enquiry embraces the construction of mathematical models of the middle ear, based upon real data, whose complexity is progressively increased to allow physical insights to be formed by means of analysis and comparison. This progression in complexity is a feature of what might be seen as a secondary conceptual aim, which is to systematically exploit the notion that a set of model equations may be viewed as a subset of a wider and more general formulation. This technique has been used to some advantage in a companion thesis devoted to the explication of the notion of simplicity as traced by the dynamics of mechanical hopping toys, Wright(2002).

With the above factors in mind it is hoped this thesis will contribute to the general understanding of the action of the middle ear, particularly in pursuit of the medical imperatives of therapeutics and prosthetics.

1.2 Outline of thesis

The outcome of the aims outlined above is to be found in the four separate papers, listed at the end of this section, which draw upon a number of technical issues treated in the following chapters. These chapters seek to provide the necessary background assumed by the papers which for reasons of brevity or repetition cannot be included within the more circumscribed format of a scientific paper.

In pursuit of this underpinning role, chapter 2 provides an abbreviated review of the anatomy of the middle ear sufficient for the purposes of defining specific biological terms used throughout the thesis, as well as providing an indication of current research in the area. Chapter 3 discusses the varieties of mathematical modelling invoked during the course of the analysis and moves on to consider the various idealisations involved in mathematically visualising and symbolically mapping the physical reality of the middle ear. Chapter 4 deals with the manipulations needed to transform the available physical data into such a state that it can be applied to the symbolic models. It also examines the programming and numerical needs required to solve the equations, derive secondary quantities and provide graphical interpretation of the answers as well as listing the equations of motion in their numerical form.

Although each paper has its own set of specific conclusions, chapter 5 takes a broader view of the matter and produces a more general set of conclusions upon which suggestions are based as to further topics for fruitful research.

The papers submitted are:

- 1. Modelling of the ossicular chain
- 2. Ossicular vibrations and the fixed axis hypothesis
- 3. The role of nonlinear dynamics of the middle ear
- 4. The effects of unilateral and bilateral constraint changes in mechanical systems: A paper in support of the study of nonlinear mechanisms in the middle ear

Papers 1- 3 hve been submitted to the *Journal of Biomechanics* as, 'The biomechanics of the middle ear, parts I, II and III', respectively.

1.3 Statement of authorship

All theoretical and computational results together with their interpretation and the writing of this thesis, have been undertaken solely by Thomas Wright.

Chapter 2

The Middle Ear

This chapter outlines the basic anatomy and function of the middle ear within the wider contexts of the science of hearing and its physiological setting. In view of the complexity of issues encountered only those elements deemed strictly relevant to the understanding of this thesis will be discussed, although references are provided for items deemed of particular interest.

2.1 Anatomy

As might be inferred from its name the middle ear is the functional unit of the auditory system which stands between the outer ear and the inner ear. In figure 2.1(a), the outer ear is that portion which includes the visible pinna and auditory canal, whilst the inner ear is the cochlea and its associated structures. The middle ear's function is to convert the vibrations of the sound air pressure waves, collected and channeled by the outer ear, into near-water like pressure waves in the cochlea. Here the fluid's motion is detected by hair cells which convert it into electrical impulses for onward transmission via the auditory cortex to the brain for processing. In this light the middle ear's function is that of a transformer whose outer boundary is defined by the eardrum or tympanic membrane, and whose inner boundary by the oval and round windows schematised in figure 2.1(b). Interposed between these two elements is the middle ear cavity which houses the transforming mechanism, the ossicular chain, a linked chain composed of the smallest bones in the human body, the malleus, incus and stapes.

This sound transmission pathway is not the only route available for sound to reach the cochlea, if a vibrator is applied to the skull the cochlea can be stimulated directly without the need for the intervening middle ear structures. Although of importance from the point of view of medical diagnosis and prothesis possibilities, this mode of sound transmission will not be discussed further.

2.1. ANATOMY 5

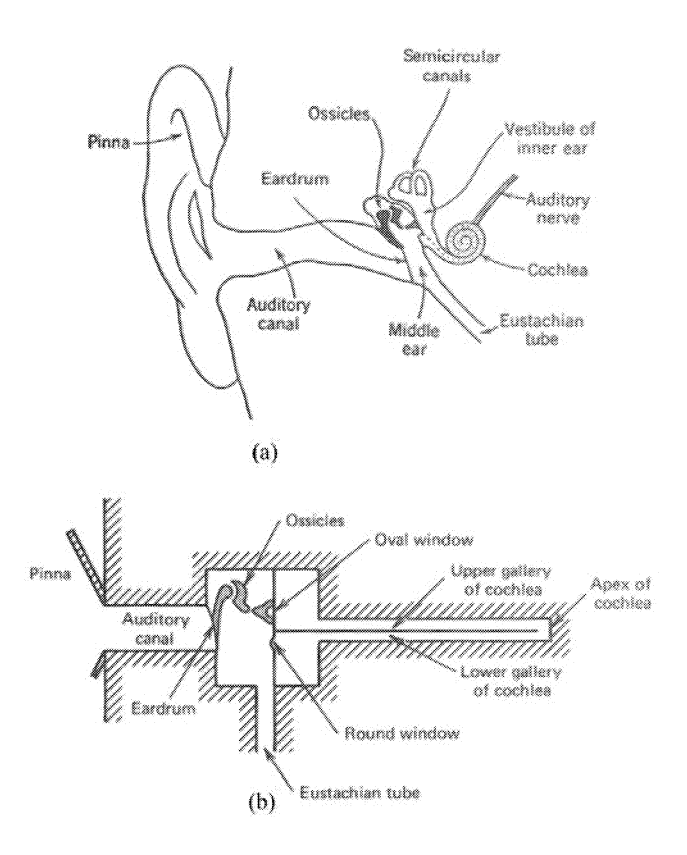


Figure 2.1: (a) Human auditory system, (b) Schematic diagram of auditory system, Kinsler L.E., et. al. (2000)

Figure 2.2 shows in more detail the anatomical structure of the middle ear and its various components. The ossicular chain vibrates in the middle ear space which is ventilated to the ambient external air pressure via the Eustachian tube to the throat. This tube is normally kept closed but can be opened by means of muscles near the throat allowing the ambient pressure on either side of the tympanic membrane to be maintained. In this fashion only the small pressure variations created by the impingement of sound waves upon the membrane are sensed and transmitted. The function of the Eustacian tube is most easily seen when a person experiences a relatively significant change in ambient pressure in a short time as in a pressurising aircraft. Here the act of yawning or swallowing causes the muscles of the Eustacian tube to open, equalise the pressure across the membrane and reduce what can be significant pain.

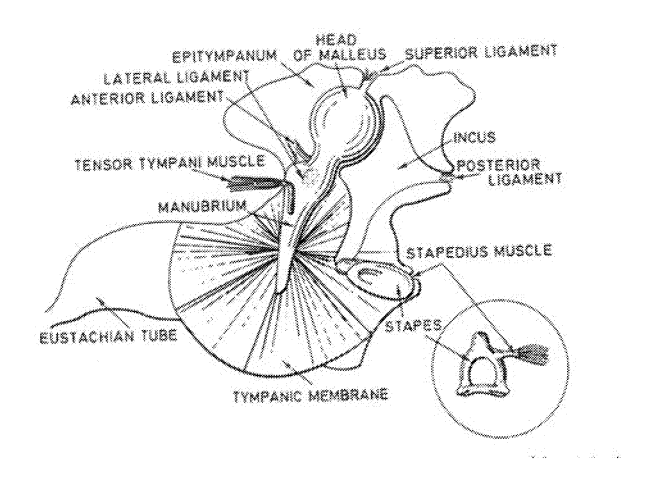


Figure 2.2: The middle ear viewed from stapes footplate. Møller(1970)

2.1.1 The tympanic membrane

The typanic membrane or ear drum is a conically shaped construct with radial fibres running from the centre to the periphery overlaid with a second set of ring fibres. The distribution of material is not uniform with most of the strength being concentrated at the centre whose point of maximum curvature is called the umbo.

2.1.2 The middle ear cavities

Although the middle ear cavity is referred to in the singular the void is much more complicated than this and is usually described as being composed of three adjacent volumes, the cavum tympani, the epitympanum and the pneumatic cells. From the present perspective these three groups will be treated as a single coherent space.

2.1.3 The cochlea

It is not the intention to deal with the mechanics or construction of the cochlea beyond noting its function and drawing attention to the oval and round windows schematised in figure 2.1(b). The oval window is covered by the footplate of the stapes whose periphery is joined to the periphery of the oval window by the annular ligament which acts as a flexible seal. The round window is simply a membrane covered opening into the middle ear cavity whose function is to flex as the pressure waves in the cochlea are generated at the oval window, thus acting as an energy absorber.

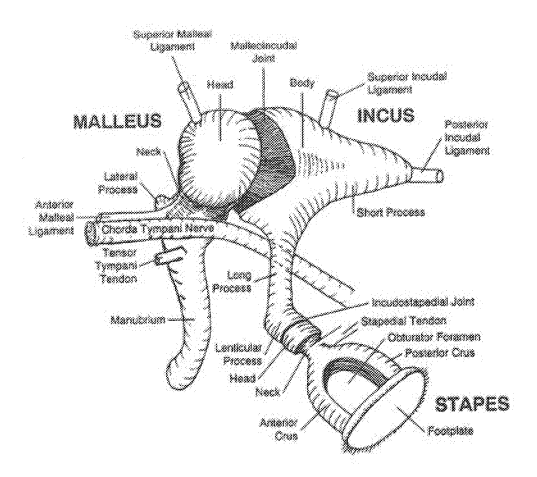


Figure 2.3: The ossicular chain viewed from the stapes footplate with tympanic membrane removed. Yost(2000).

2.2 The ossicular chain

From figure 2.2 it will be seen how the ossicular chain is fastened and orientated with respect to the tympanic membrane and oval window, whilst figure 2.3 shows in greater detail the three bones and some of their more important parts. Figure 2.3 is orientated with the footplate of the stapes visible but the tympanic membrane removed. The figure also shows the method of suspending the chain from the cavity walls and draws attention to the fact that the space is also traversed by the chorda tympanic nerve. Since the geometry of the chain will be examined in considerable detail in the next chapter only the most basic of descriptions will be offered here.

The malleus (hammer) has two principal parts, the manubrium and its rounded globular head. Apart from its fixing to the tympanic membrane the malleus is supported by the anterior malleal ligament, the superior malleal ligament and a ball and socket joint, the incudo-malleal joint; the manubrium also has attached to it the tensor tympani muscle. In terms of the functioning of the malleus, the superior malleal ligament is judged to be slack and viewed as primarily a means of supplying nutriments to the incudo-malleal joint The incudo-malleal joint is a true diathrodial joint, in that it is a true ball and socket joint, encased in ligamentous tissue and lubricated by synovial fluid.

The incus (anvil) is linked to the malleus by the incudo-malleal joint and is supported by the superior incudal ligament, the posterior incudal ligament and another diathrodial joint, the incudo-stapedial joint, linked to the stapes. Like the superior

malleal ligament, the superior incudal ligament is judged to have a non-suspensory role, the suspension function being taken up by the posterior incudal ligament and the two joints.

The third bone in the linkage, the stapes (stirrup) has its neck fixed to the incudo-stapedial joint's capsule and its footplate fitted into the oval window of the cochlea. Attached to the head of the stapes is another muscle, the stapedius muscle whose point of attachment can vary somewhat towards and including the lenticular process.

Although the presence of the two muscles in the middle ear complex, has always been acknowledged, their actions and raison d'etre are not as clear as might be supposed. It is known that the action of the stapedius muscle is linked to the onset of the acoustic reflex which acts to attenuate or reduce the amount of sound energy reaching the cochlea in the presence of high sound pressures. Such pressures are normally generated by strong impulses, but whether the reflex is a protective device or not is still a matter of unsettled debate. Similarly the function of the tensor muscle is also obscure although it is generally accepted that it works independently of the stapedius and is not active in the initiation of the acoustic reflex. The common view is that it is a tensioning device working in some way to maintain optimal transmission charcteristics for the chain.

2.3 The working of the middle ear and the fixed axis hypothesis

From the above descriptions and diagrams the mode of operation of the middle ear will be clear; the oscillation of the air molecules adjacent to the tympanic membrane cause it to oscillate. This motion is transferred via the ossicular chain to the stapes which acts as a piston oscillating in the cochlea. The middle ear's function is thus to transform pressure oscillations occurring in a very light density fluid, air, into pressure oscillations in a fluid of near-water density. The generally accepted and taught explanation of the action of the ossicular chain Yost(2000), is that the incudo-malleal block rotates about the ligamental axis which is effectively fixed. This explanation is labelled here as the 'fixed axis hypothesis'.

In the language of acoustics/electrical engineering, discussed in chapter 3, the middle ear is viewed as an impedance matching device matching the inpedance of air, to that of water. The device's biological presence is an evolutionary adaption enabling a primitive vibration sensing / hearing organ developed by sea bound life, to sense sound in air. All mammals possess middle ears of the same general description and layout as man's although their individual arrangements and sizes vary with the size of the animal, Nummela(1995). This similarity has meant that most live data has been collected from experiments conducted upon animals, particularly cats, or

from non-invasive human experiments as well as post-mortem human specimens.

2.4 Sound measurement

It is well known that for many physical effects impacting upon the human senses, it is easier to perceive differences in signal intensity at lower absolute levels than at higher ones. By means of integration this can be shown to result in a logarithmic relationship defining a specific intensity level with respect to an agreed standard. Although there are a number of definitions used in hearing acoustics the standard employed here is the Sound Pressure Level (SPL) relationship given by:

$$SPL = 20\log_{10}\frac{p}{p_o}$$

In this expression SPL is measured in decibels dB, p is the pressure variable and p_o the international reference standard defined as $p_o = 20\mu Pa$. This reference standard is the experimentally determined minimum pressure required by an average young adult to be able to detect a sinusoid in the 1000 to 4000Hz range.

Figure 2.4 shows the frequency response of the human ear to sound intensity ex-

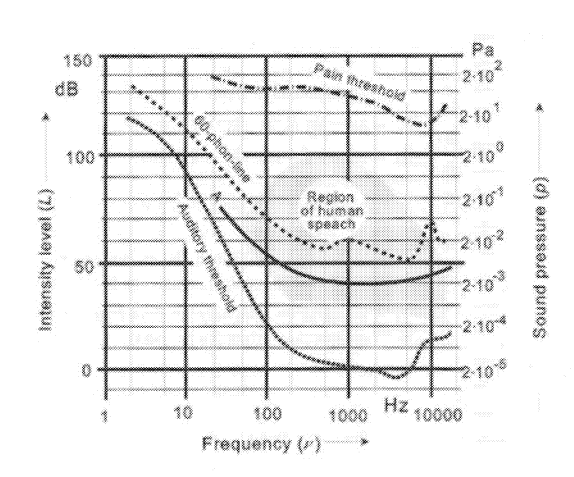


Figure 2.4: Response of the human ear to sound intensity. GlaserR, (2001).

pressed in both absolute pressure units Pa and SPL whilst figure 2.5 illustrates various types of common noise as expressed on the SPL scale. For the sake of brevity, further discussion of units and the order of magnitude of the various quantities involved as both variables and parameters, is deferred until chapter 4.

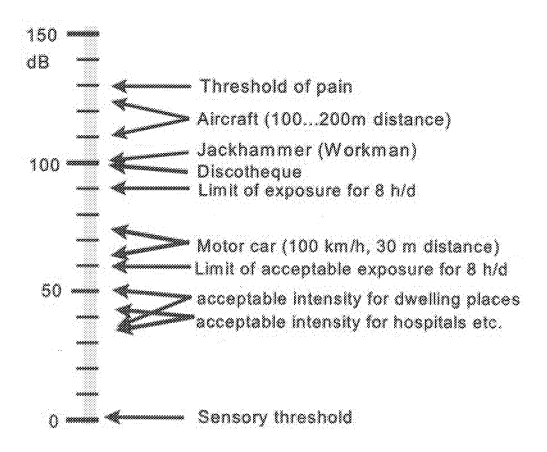


Figure 2.5: Noise levels from different sources. GlaserR, (2001).

2.4.1 Hearing loss and prosthesis

Most normal disorders of the middle ear are connected with infections, particularly in children, which affect the middle ear cavity and tympanic membrane; usually they are temporary and treated with antibiotics. More radical treatment, usually surgery, is required for problems concerned with the ossicular chain such as otosclerosis, where a bony outgrowth of material around the oval window renders the footplate of the stapes immobile. This is treated by removing the stapes, or part of it and fitting a prosthesis in its place. Similarly the ossicles can be fused together, ossicular fixation, either as a congenital or progressive condition, which depending upon circumstances may require the ossicle to be removed and replaced by a prosthesis. Similarly the joints in the chain can break, ossicular discontinuity, which may or may not require a prosthesis.

From the above it will be seen that the use of prostheses in correcting mechanical problems associated with the ossicular chain is a relatively well understood procedure, however the design of such devices is still subject to improvement, Hersh & Johnson (2001).

2.5 Current research interests

It is reasonable to say that the vast majority of investigations relating to the middle ear are experimentally driven; since measurements are extremely difficult to make and technically demanding new results are constantly being reported as yet more delicate data sensors are brought to bear. The theoretical grounding for much of this work has been based upon the assumption of the middle ear's motion being planar.

Since the 1980's there has been an increasing number of studies which have moved to the opposite theoretical extreme having modelled a combination of the middle and outer ear by means of finite element techniques. Of this work most has been devoted to describing the complex behaviour of the tympanic membrane detached from its onward transmission chain. Others have modelled the complete chain and in the process have generated data on materials that previously was lacking, Koike & Wada (2002). Having noted this other researchers have continued to use the more traditional Zwislocki type electrical analogues discussed in the next chapter as their basic means of investigation, generating transfer functions and improving their techniques of coefficient estimation Pascal & Boureade(1998).

Nearly all the theoretical work (with the exception of tympanic membrane studies), has been undertaken under the assumption of linearity and where nonlinearity has been invoked it has been associated with nonlinear 'curve fitting'. As far as is known, the technique adopted here of developing three dimensional multi-rigid body models whose complexity and computing requirements stand between simple two dimensional models and very large finite element constructions is one that has received almost no attention from contemporary researchers. Only one relevant paper has been located Hudde & Weistenhöfer(1997); and that is mainly devoted to an exposition of adapting network techniques to three dimensional ossicular motion, the authors noting the lack of suitable data to fit into the model.

Unlike much current work, the present thesis seeks to investigate the validity of some of the fundamentals of the middle ear's operation that seem to be taken for granted by most investigators. This includes such issues as the presence, or not, of linearity and the validity of currently accepted expanations of the ossicular chain's behaviour.

Chapter 3

Model constructs and multibody dynamics

In approaching the modelling of the middle ear there are a number of choices available, each with their own disciplinary conventions, in which to graphically and conceptually express the equations of motion. This chapter briefly outlines these types and also considers the idealizations and techniques used in the derivation of the equations of motion and the interpretation of their results.

3.1 Conceptual approaches

3.1.1 Electrical analogues and network theory

The history of investigations into the mechanics of the middle ear has since the mid- 1950s been dominated by the use of electoacoustic analogues. This is due principally to the close relationship existing between alternating current theory and acoustic/wave systems via the use of linear, small wave approximations and their pivotal role in transducer theory. The method is particularly well suited to act as a theoretical foundation due to its, simplicity and ease of incorporating directly measured data of different types. These different data such as fluid and rigid body motions are reduced to common units of electoacoustic measurement, such as acoustic ohms (Ω) and acoustic Henrys (H), which can then be manipulated by means of electrical network theory.

All middle ear electroacoustic analogues are based upon Zwislocki's (1962) scheme which is illustrated as a functional arrangement in figure 3.1. Here it will be seen that the anatomical functions discussed in chapter 2 are visually represented by a Kirchoffian linear network with its components disposed in parallel and series combinations mirroring the underlying mathematical structure inherent in such relationships

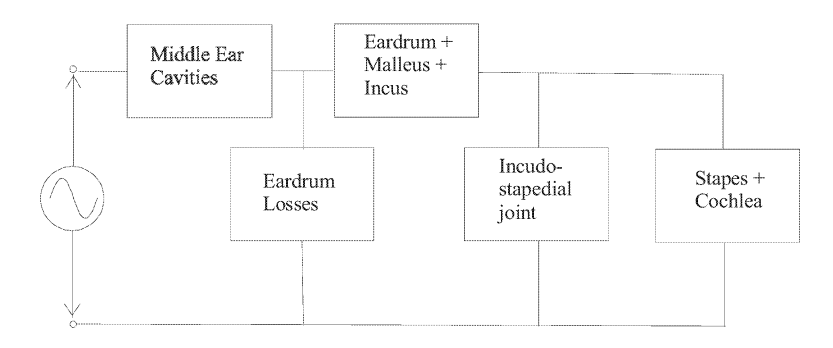


Figure 3.1: Zwislocki's electroacoustic model(1962)

The analogies that exist between mechanical and electrical quantities are well known. Although two such analogies are found in common use, the force/voltage and the force/current, the force/voltage analogy will be used here. That is, the mechanical quantities of linear displacement q, velocity \dot{q} , mass m, spring constant k and viscous resistance c are analogous to charge, current, inductance, the inverse of capacitance and resistance, respectively. These analogies and their equivalently derived quantities such as force and power are treated in standard texts such as Raven(1968), as is the technique of graphical translation between the two visualisations.

The normal method of using these electoacoustic analogues is to invoke the Zwislocki representation as the underlying mathematical structure, conduct experiments and then add or adjust components to fit the data, as for example in Lutman & Martin (1979) and Pascal & Boureade (1998). In most cases the individual components such as inductances are treated as constants, so that the network as a whole is linear with nonlinear elements being incorporated as necessary.

Although any analogical relationship is simply the outcome of the form of fundamental equations governing the fundamental processes it is necessary in considering such matters to decide at the outset upon the type of visual method to be used in expressing these relationships. The form chosen for this thesis is not the electroacoustic visualization but the mechanical.

A major reason for this decision is that since the movement of the ossicular chain will be the focus of attention and since that movement will be undertaken in three dimensions, the linearity and/or nonlinearity will be heavily influenced by cross coupling of terms in the equations which renders conventional network symbolism difficult to construct and analyse. Variants such as bond graph formalism require further special symbols and indeed when the method is invoked to visualize

mechanical systems, the mechanical representation is invariably drawn first from which the bond graph is then drawn from which the equations of motion are derived, Karnopp et al (2000).

At the root of the use of electro/acoustic analogues is the concept of impedance it already having been noted that the middle ear is usually regarded as an impedance matching device matching the impedance characteristic of acoustic wave transmission in air and water. Impedance is simply the alternating current version of direct current resistance, which due to the sinusoidal nature of alternating current introduces an extra phase angle into its working. Thus if Z is the impedance measured in Ω , I the alternating current in amps and V the alternating voltage in volts, $Z = \frac{V}{I}$. The equivalent mechanical analogue is therefore the mechanical impedance given by $Z_{mech} = \frac{F}{v}$ were F = force and $v = \dot{q}$ =velocity. There is no particular reason for using impedance in predominantly mechanical systems since its use is based upon electrical usage where current, the time rate of change of charge is more accessible than the charge itself, whereas in mechanics displacement q is the accessible variable and velocity \dot{q} the secondary quantity.

The principal reason however for invoking a mechanical as opposed to a network representation lies in the sense of physical geometry and kinematics that is entailed in developing and using the method. It is felt schematic mechanical diagrams aid the process of understanding more readily than electrical circuits due to the incorporation of geometrically visual elements even if those elements are themselves following stylised conventions.

For reasons which will be discussed in section 3.2 below, paper 1 takes a well known and frequently quoted network model, Kringlebotn(1988), and uses it as an initial basis for investigation. This network is then converted into a mechanical representation where it is felt the schematic geometrical layout provides a more intuitive feel as to the nature of the idealizations involved and indeed highlights the basic physical reasoning underpinning the model.

3.1.2 The classical mechanics of constrained systems

There are an embarrassingly large number of theoretical methods available for deriving the equations of motion of systems composed of particles and bodies forming a chain. Each method possesses particular nuances, specialized language and conventions. The view taken here is that the fundamental laws governing the motion of matter are those expressed by Newton which at their heart define for a particle (itself an idealisation), the equality of force to the rate of change of linear momentum. This particle law and its extension to the further idealised singular multi-particle rigid body which is both translating and rotating in a three dimensional Euclidean space and due to Euler, forms the basic tool for equation formation. The resulting Newton/Euler force- rate of change of momentum, balance equations require no

extra hypotheses for their formulation.

The extension of the Newton/Euler laws to account for multiple bodies connected to each other, driven by external forces and held together by forces transmitted between them whose equality and opposition are the subject of Newton's third law, is the subject of multi-rigid body dynamics. The extension to the case where some of these bodies are constrained to move in particular ways brings no particular conceptual difficulties into play but does lead to large practical difficulties in the solution of the equations. Further since the Newton/Euler equations involve all the forces generated, including those connecting the individual bodies to each other and those maintaining the constraints, a lot of information and calculation is required to produce results that are unnecessary if only the gross motions of the bodies are required.

To overcome this constaint force problem the well known Lagrange/D'Alembert hypothesis is invoked which postulates that the force of constraint reaction is normal to the direction of motion so that no work is done by the constraint. This procedure is undertaken in symbolic form in paper 1 to produce D'Alembert's equations. It is important to note that the Lagrange/D'Alembert hypothesis is just that and its application is not only a simplifying procedure but also an unproven assumption, particularly where biological systems are concerned.

Although the detailed issues attached to the generation of the various equations of motion are dealt with below in section 3.2, the actual equations of motion generated are so large that they are difficult to discuss as particular entities within the papers. To enable this to be done the equations are invoked in their symbolically explict coupled form, thus:

$$\sum_{i=1}^{n} m_{ij} \ddot{q}_{j} + \sum_{l=1}^{n} \sum_{m=1}^{n} [i, lm] \dot{q}_{l} \dot{q}_{m} = -\frac{\partial V}{\partial y_{i}} - \frac{\partial R}{\partial \dot{y}_{i}} = F_{i} \quad i = 1 \cdots n$$
 (3.1)

Here the m_{ij} are generalised masses, the [i,lm] Christofell's symbols of the first

kind, V and R the potential and Rayleigh functions respectively and F_i the generalised force corresponding to the generalised coordinate q_i with i running from 1 to n.

These equations, although normally associated with Synge's (1926) derivation of Lagrange's equations hold regardless of the method used to arrive at them whether it be D'Alembert, Lagrange, Hamilton etc, providing the coordinates, frames and parameters are the same. Thus the equations put into their indicial form are perfectly general and have the merit of allowing direct entry into the geometry of the motion via the language of differential geometry, configuration spaces, holonomic constraints, Reimannian geometry, generalized coordinates, generalized forces and

16

generalized momentum, whilst still retaining an essentially Euclidean vector based orientation.

To avoid over complication, the use of 'modern' geometrical language as currently employed in mathematical physics and now gradually entering engineering usage, Block et al (2000), will not be used here. Thus as fruitful as the concepts of differential manifold, fibre bundles, Lie derivatives, Lie groups, differential forms and the operations associated with them are, this work will remain within the explanatory base of what might be considered engineering mechanics.

3.1.3 Screw theory

Paper 2 is an examination of the fixed axis hypothesis, briefly referred to in section 2.3. To undertake this examination elements of screw theory are used and although the theory has received application within the robotics community over recent years, it is not a theory that may be considered to lie within in the mainstream of dynamical activity. The history of the subject stretches back to Euler and had a sufficiently well defined mathematical structure by the early 20th century to be capable of dynamical application, Ball(1998), even if its use has tended to remain restricted within the area of kinematics.

The presentation in paper 2 is meant to be as self contained as possible and in-

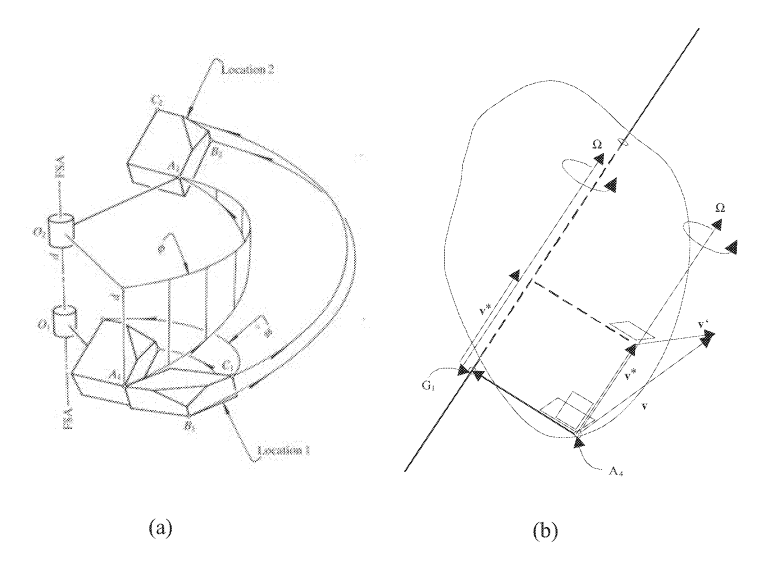


Figure 3.2: (a) Finite screw motion, Phillips(1990) (b) Instantaneous velocity screw

cludes reference to a set of basic explanatory texts dealing with screw theory. The

fundamental idea is that illustrated in figure 3.2(a) where a rigid body moves in three dimensional space from location 1 at time t_1 to location 2 at time t_2 . It is shown in Bottema & Roth (1979) that to do so a unique line exists, the screw axis, line FSA in figure 3.2(a), around which the body simultaneously translates a distance d and rotates an angle ϕ during the period $\Delta t = t_2 - t_1$. Figure 3.2(a) illustrates the large finite displacement case, but as $\Delta t \to 0$ it is easily seen that in the instantaneous limit the direction of the axis of the line is defined by the direction of the angular velocity vector. Figure 3.3(b) illustrates this limit where the instantaneous movement is composed of a rotation around the axis and a linear velocity in its direction. It is easily shown that the velocity along the axis is the body's minimal linear velocity component.

Figure 3.2(b) illustrates for a general case how for a known linear and angular velocity acting at point A_4 , an non-unique reference point through which the rotational axis passes is given by the point G_1 . This point is defined by the radius vector $R_{A_4G_1}$ equation 3 in paper 2, where in figure 3.2(b) \mathbf{v} corresponds to $u_4\mathbf{n}_1$ of the equation.

Given that the motion of the body in time is known through the solution of the equations of motion, the linear velocity and angular velocities can be derived for all points in the body and the non-unique position through which the screw axis passes can be derived as a function of the movement of the body. The surface traced out by this axis is known as the axode.

Although the example given above is concerned with the screw defined with respect to body movement an analysis for linear force and torque reveals a similar screw arrangement for these two quantities. In common with other writers and in the interests of clarity, the screw which is the combination of the linear velocity and angular velocity vectors will be called a velocity screw and the screw associated with the force and torque will be called a force screw; this is a departure from Ball's designation of 'twist' and 'wrench' respectively.

3.2 Derivation of equations of motion

Although papers 1-3 seek to trace out a progressive approach in addressing the dynamics of the ossicular chain by invoking three separate models working from the simple to the complex, the approach taken below in describing the formation of these three equations follows the reverse route. Since the methodological concept adopted in this work is to view the simple as a subset of the complex, the generation of the equations of motion for the full three dimensional set will be considered to cover all the other equations with particular issues relating to any particular set being discussed as required.

3.2.1 Underlying approach

Paper 1 shows how the two dimensional model of Kringlebotn (1988), a variant of the Kwislocki formulation, is converted into three dimensions by retaining those elements relating to the tympanic membrane and the cochlea, but 'subtracting' the two dimensional representation of the ossicular chain and inserting in its place the three dimensional form. This three dimensional representation is shown in figure 3.3, which is a redrawn and combined figure derived from the original basic data set Weistenhofer & Hudde (1999), discussed in more detail below.

It will be seen that figure 3.3 shows the incus and malleus as a single fused block

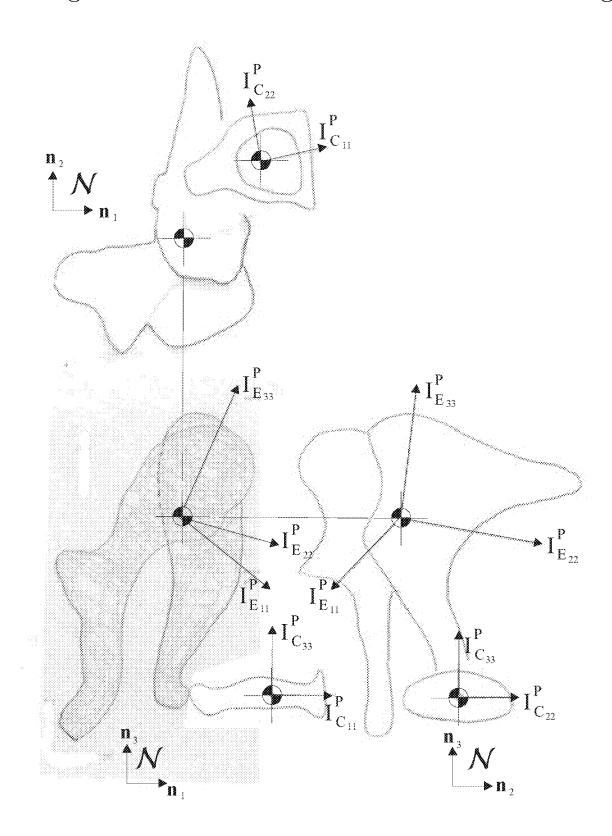


Figure 3.3: Basic ossicular chain configuration, scale 1 unit vector = 1mm. Adapted from Weistenhöfer & Hudde(1999)

with its centre of mass at the putative incudo-malleal joint. Since the behaviour of the chain with both incus and malleus moving relative to each other with the joint in operation is a major interest of this work, this 'fused' data has to be converted into separated dynamical data. This operation is discussed below in chapter 4, so that for the present it may be assumed that the centre of masses of both the incus and malleus are known in addition to the data symbolized by figure 3.3.

3.2.2 Geometry and configuration

Figure 3.4 shows the schematic rigid, massless, idealised frame work imposed upon the basic geometrical data of figure 3.3 with the malleus, incus and stapes denoted by calligraphic A, B and C and points upon them by the roman A_1 etc. In this scheme it will be seen that the centre of masses of the mallues, incus and stapes are denoted by A_1 , B_1 and C_1 . The incudo-malleal joint is denoted by the point A_2 which since it is a joint coincides with the incus's point B_2 . Point A_4 is that point, defined by Kringlebotn, as the 'effective attack point' on the manubrium, which possesses the same velocity as the eardrum as a whole and which approximates very closely to the motion of the umbo. Point A_3 is the point at which the anterior ligament is attached to the malleus whilst B_3 is the point of attachment of the posterior ligament to the incus and B_4 the point of attachment of the incudo-stapedial joint to the incus. Unlike the incudo-malleal joint the incudo-stapedial joint is deemed to possess relative motion in both rotational and translation modes so the point of attachment of the joint to the stapes C_3 does not in general coincide with B_4 . Point C_2 on the stapes coincides with the geometrical centre of the stapes footplate.

Figure 3.5 shows the overall schematic dynamical model from which the equations of motion are generated, the elements within it being an amalgamation of figures 3.4 and one dimensional elements taken over from the Kringlebotn model. The model is shown in its equilibrium position (the state implicit in figure 3.4) with a Newtonian right angled reference frame and directional triad, $\mathbf{n}_1, \mathbf{n}_2$ and \mathbf{n}_3 , anchored to the fixed point 0, which for purposes of visual clarity and coordinate definition is illustrated in the 'opened up'position, that is $z_1 \cdots z_4$ should be zero

In line with the Kringlebotn model, the motion of points A_4 and C_3 are unidirectional as defined by \mathbf{n}_1 , their respective lines of action being separated in three dimensional space as shown. Thus the eardrum, ear cavities, eardrum suspension, and cochlea are modelled as particles m_1, m_2, m_3 and m_D which move in one dimensional motion, whilst the ossicular chain's components moving in three dimensions, are interposed between them.

For the purpose of generating the equations of motion it is necessary to define the dynamical and geometrical properties of the ossicular bodies which in turn require the definition of frames of reference which are themselves defined with respect to the basic Newtonian set \mathcal{N} . Thus in accordance with figure 3.6 reference frame \mathcal{A} and its associated triad $\mathbf{a}_1, \mathbf{a}_2$ and \mathbf{a}_3 are fixed at the centre of mass of the malleus A_1 with the unit vector \mathbf{a}_2 pointing in the direction from the anterior ligament to the incudo-malleal joint. Similarly frame \mathcal{B} is fixed at point B_1 with \mathbf{b}_2 pointing from the incudo-malleal joint to the posterior ligament, such that in the

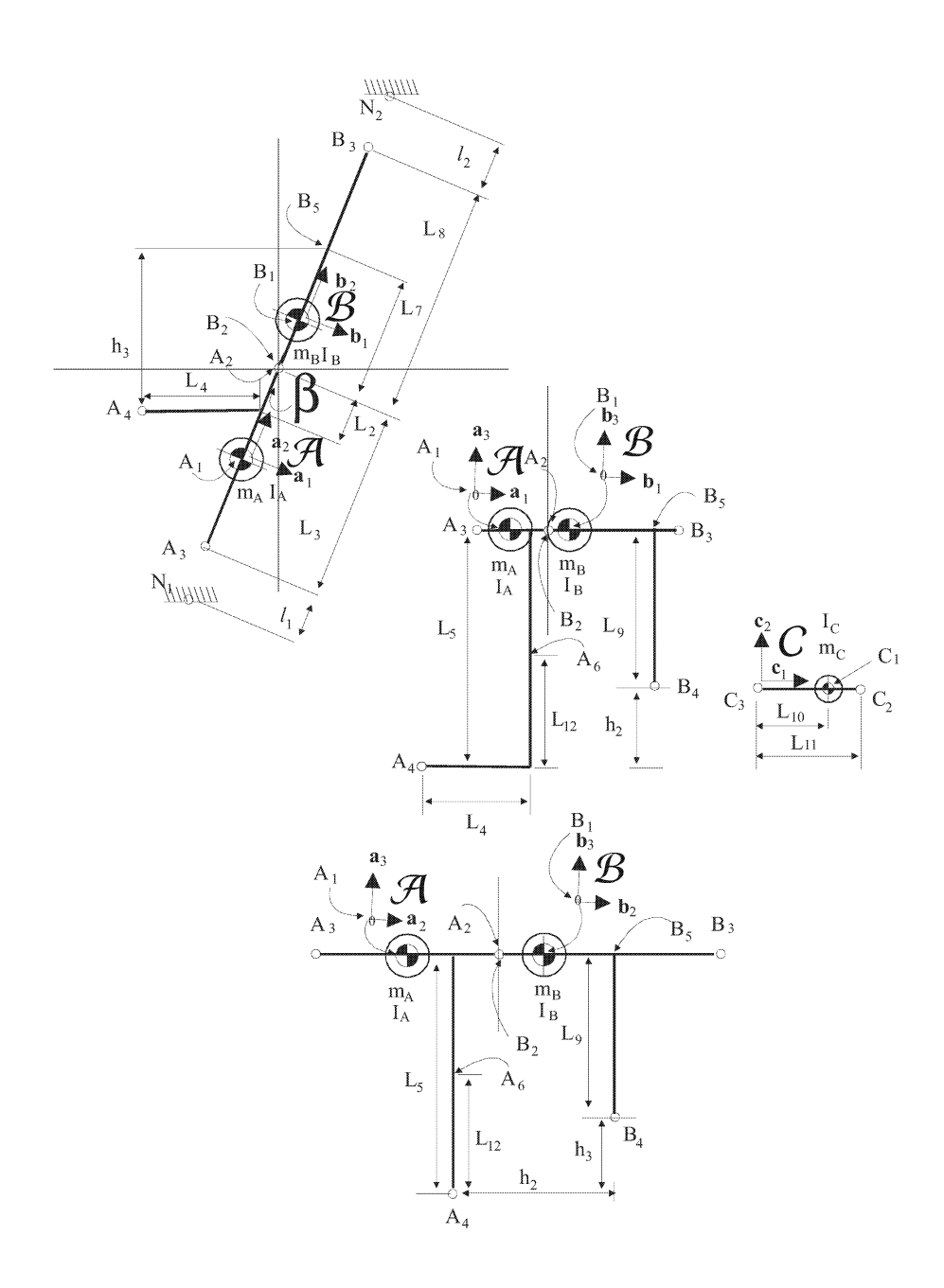


Figure 3.4: Schematic diagram of model 3 geometry

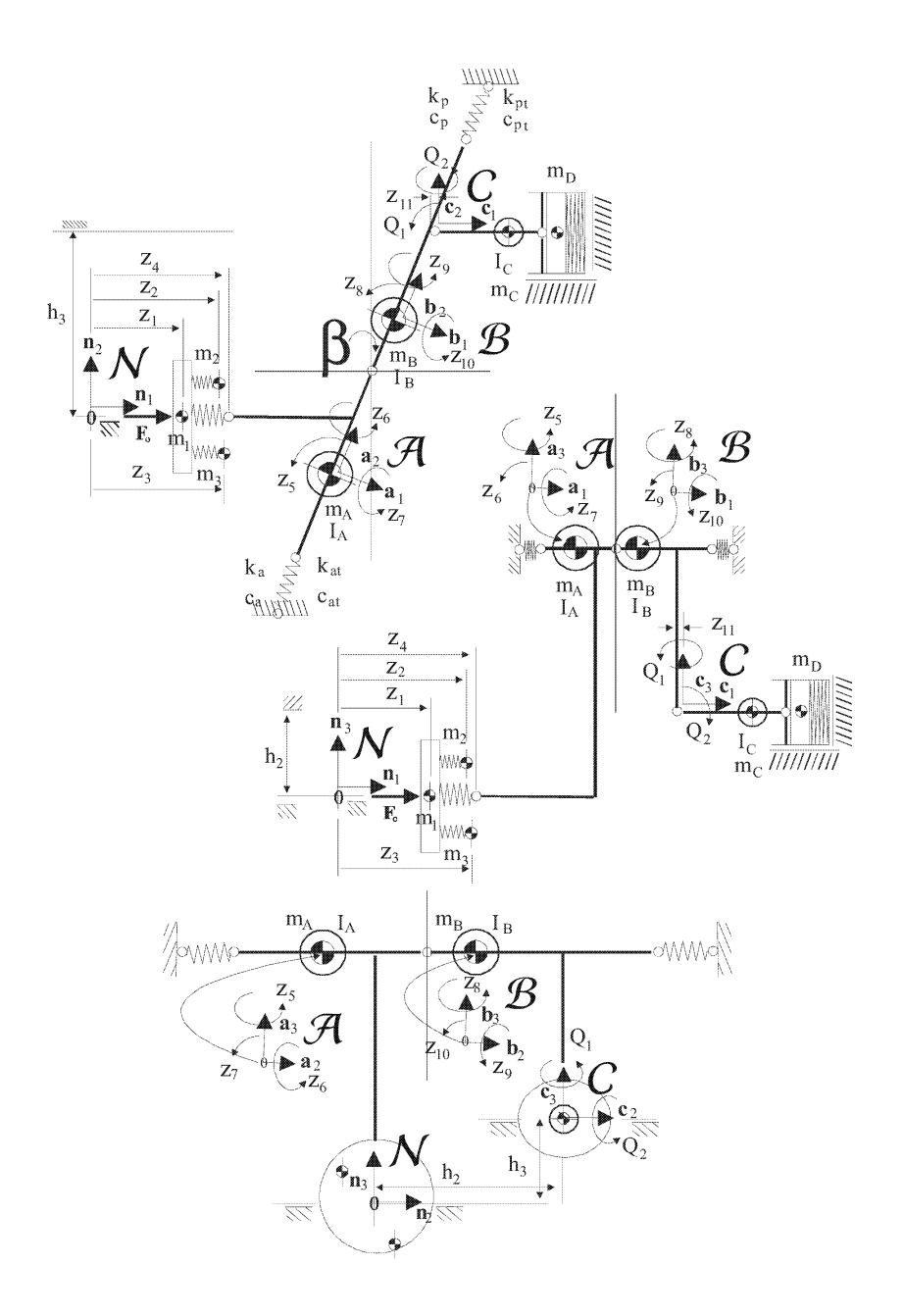


Figure 3.5: Schematic diagram, model 3

equilibrium configuration shown, \mathbf{a}_2 and \mathbf{b}_2 are instantaneously the same direction. The stapes frame C, unlike the other frames, is not anchored at it centre of mass but at point C_3 with \mathbf{c}_1 pointing along the stapedial direction from point C_3 to C_2 , with the centre of mass C_1 being fixed as shown.

To relate the positions of points, measured on the three bodies, to the same points

measured in inertial space \mathcal{N} it necessary to define the angular orientations of frames \mathcal{A}, \mathcal{B} and \mathcal{C} . Figure 3.6 shows diagrammatically these relationships by utilizing angular coordinates and intermediate frames. Thus as illustrated in figure 3.6 (a), frame \mathcal{A} , defining the angular orientation of the malleus is related to \mathcal{N} by means of the transformations, $\mathcal{N} \to \mathcal{A}^1 \to \mathcal{A}^2 \to \mathcal{A}^3 \to \mathcal{A}$. Here frame \mathcal{A}^1 is defined by the angle $+z_5$ measured in the $\mathbf{n}_1 \wedge \mathbf{n}_2$ plane such that \mathbf{n}_1 is rotated to \mathbf{a}_1^1 , about \mathbf{n}_3 ; frame \mathcal{A}^2 is similarly defined by the angle $-\beta$ which is measured in the $\mathbf{a}_1^1 \wedge \mathbf{a}_2^1$ plane $(\mathbf{n}_1 \wedge \mathbf{n}_2)$ in the negative sense about $\mathbf{a}_3^2(\ \mathbf{a}_3^1,\mathbf{n}_3)$ where β is the angle of inclination, a constant of the equilibrium configuration defining the ligamental axis. Frame \mathcal{A}^3 is defined by rotating \mathbf{a}_1^2 to \mathbf{a}_1^3 by angle z_6 as measured in the $\mathbf{a}_3^2 \wedge \mathbf{a}_1^2$ plane about \mathbf{a}_2^2 , and finally frame \mathcal{A} is related to \mathcal{A}^3 by rotating \mathbf{a}_2^3 to \mathbf{a}_2 by $+z_7$ about \mathbf{a}_1^3 (\mathbf{a}_1). Using these angles the complete transformation matrix relating \mathcal{N} to \mathcal{A} and the inverse \mathcal{A} to \mathcal{N} can be derived by standard techniques. The transformation $A^1 \to A^2$ using β has been included to underline the importance of β as an individual parameter of the geometry although the combined effect of applying z_5 and β is of course the angle $z_5 - \beta$ which could have been made a coordinate in its own right if so wished.

Unlike frame \mathcal{A} frame \mathcal{B} is defined in figure 3.6 (b) not with respect to \mathcal{N} but with respect to frame \mathcal{A} defined in figure 3.6(a). The same routine as with frame \mathcal{A} is followed in order to define frame \mathcal{B} using the angular coordinates $+z_8$ to define \mathcal{B}^1 with respect to \mathcal{A} , $+z_9$ to define \mathcal{B}^2 with respect to \mathcal{B}^1 and $+z_{10}$ to \mathcal{B} with respect of \mathcal{B}^2 , allowing the transformation matrix relating \mathcal{A} to \mathcal{B} and vice versa to be generated. Frame \mathcal{B} is then related to frame \mathcal{N} by the chained relations $\mathcal{N} \to \mathcal{A}^1 \to \mathcal{A}^2 \to \mathcal{A}^3 \to \mathcal{A} \to \mathcal{B}^1 \to \mathcal{B}^2 \to \mathcal{B}$.

The relationship of frame \mathcal{C} to \mathcal{N} , figure 3.6(c) is defined slightly differently to the other frames. Here \mathcal{C} is related directly to \mathcal{N} by the transformations $\mathcal{N} \to \mathcal{C}^1 \to \mathcal{C}^1 \to \mathcal{C}$ with the angle $+Q_1$ defining the relationship $\mathcal{N} \to \mathcal{C}^1$ and $+Q_2$ the relationship $\mathcal{C}^1 \to \mathcal{C}^2$, however $\mathcal{C}^2 \to \mathcal{C}$ is defined by the coordinate $+z_{11}$ which has the dimensions of length (as opposed to the previous angles), such that the transformation $\mathcal{C}^2 \to \mathcal{C}$ is a parallel transport in the direction \mathbf{c}_1^2 (\mathbf{c}_1) direction.

Thus a radius vector defining the position of, say, the stapes footplate with respect to \mathcal{N} , \mathbf{r}_{0C_2} , will as it stands involve the coordinates $z_1, z_4, z_5, z_6, z_7, z_8, z_9, z_{10}, Q_1, Q_2, z_{11}$, the individual z's being considered in the sense of Lagrangian generalized coordinates possessing appropriate angular or linear dimensions. For ease of discussion and in the absence of satisfactory anatomical terms, the aero-marine conventions

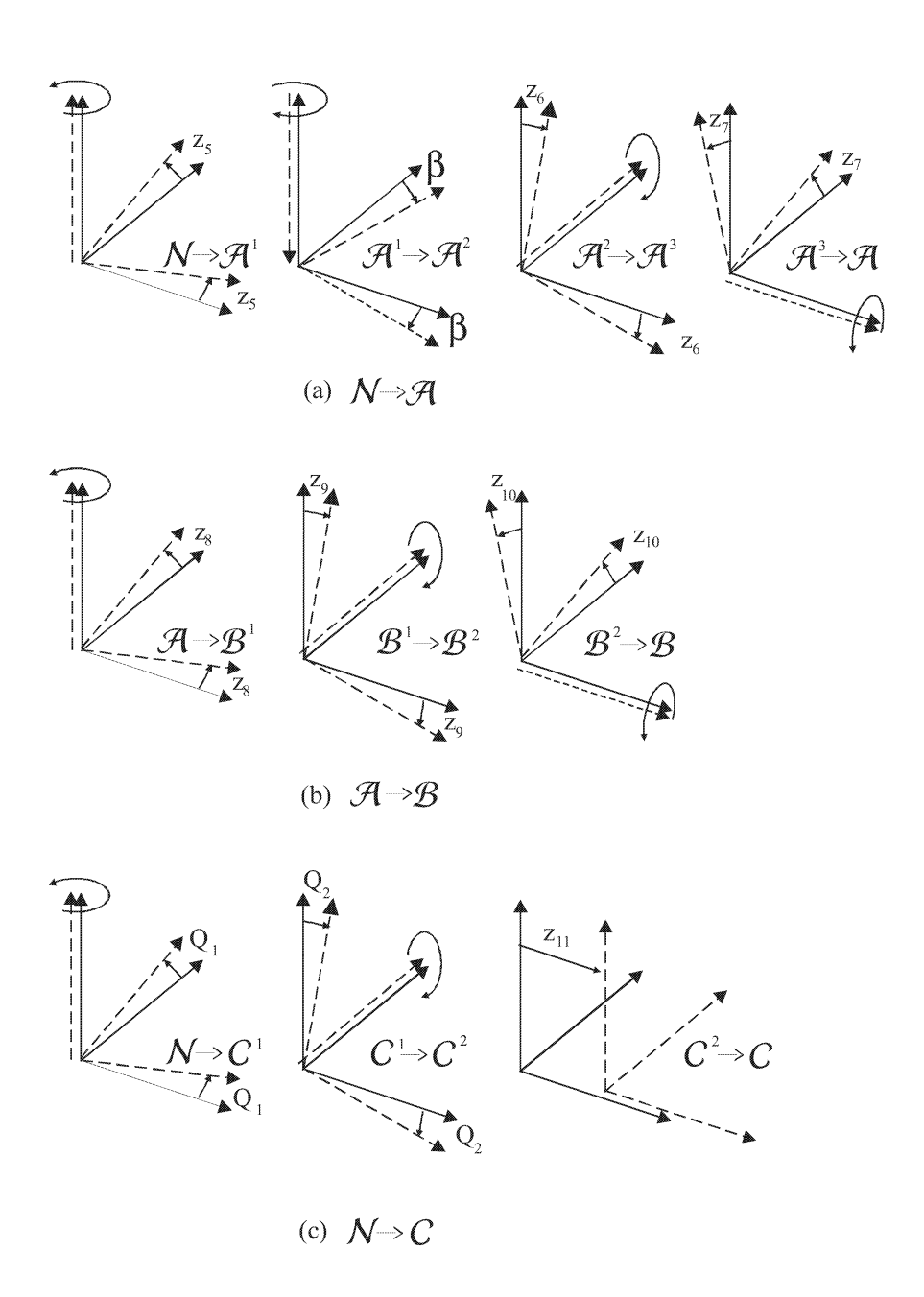


Figure 3.6: Definition of coordinate frames for model 3

relating to the naming of coordinates will be used here, thus z_5, z_6 and z_7 will be denoted as the 'yaw', 'pitch' and 'roll' angles respectively of \mathcal{A} with respect to \mathcal{N} and z_8, z_9, z_{10} as the yaw, pitch and roll angles of \mathcal{B} with respect to \mathcal{A} . Similarly Q_1 and Q_2 are the yaw and pitch angles of \mathcal{C} with respect to \mathcal{N} .

Since points A_4 on the malleus and C_2 on the stapes are confined to move in the \mathbf{n}_1 direction but on parallel displaced lines, the linked movements of \mathcal{A} , \mathcal{B} and \mathcal{C} must conform to these constraints. Given the geometry of figures 3.4 and 3.5 it will be seen that the projected positions of A_4 and C_2 on to the fixed plane $\mathbf{n}_2 \wedge \mathbf{n}_3$ are the point 0 and the point defined by the radius vector $h_2\mathbf{n}_2$ and $h_3\mathbf{n}_3$ respectively. From the geometry of the situation and taking the component forms of \mathbf{r}_{0C_2} , $(\mathbf{r}_{0C_2})_2 = h_2$ and $(\mathbf{r}_{0C_2})_3 = h_3$ so providing two constraint equations which can be used to eliminate Q_1 and Q_2 respectively. The outcome of reducing the number of coordinates in this way means that the state of the whole system is defined by the coordinate set $[z_1 \dots z_{11}]$ however it is not necessary to undertake such a reduction since the system's state can equally well be defined by the set $[z_1 \dots z_{10}, Q_1, Q_2, z_{11}]$, plus the two equations of constraint linking Q_1 and Q_2 to h_2 and h_3 if wished.

3.2.3 Equations of motion

The equations of motion of the entire system illustrated in figure 3.5 are derived as discussed in section 3.1.2 by application of the basic Newton/Euler laws of particle/ rigid body motion. Assuming Q_1 and Q_2 are eliminated via the equations of constraint, paper 1 outlines symbolically the Newton/Euler procedure, incorporating the application of the Lagrange/D'Alembert principle of idealized constraint forces. Using the principle the equations of motion are rid of the constraint forces to produce the final reactionless D'Alembert equations of motion. The only difference between the derivation of model 1 in paper 1 and model 3 as discussed here is that the latter equations are extended to take account of the separation of the fused incudo-malleus block into separate malleus and incust hereby introducing the three extra coordinates associated with this increase in complexity. The physical generation of these equations of motion was undertaken using the software package Sophia as indicated in paper 1 and discussed in the next chapter.

The derivation of the external forces, the spring and viscous dissipation forces (gravity being of no consequence in this case), proceeded by means of the construction of potential and Rayleigh functions for the system as a whole. The differentiation of these functions with respect to a given coordinate or coordinate velocity as appropriate, yielding the given generalized potential and damping forces for the respective generalized coordinate.

Since the total number of equations of motion generated is equal to the degrees of freedom of the system as defined by the eleven coordinates $[z_1 \dots z_{11}]$, the equa-

Model 3	Model 2	Model 1	2D Model
z_1	y_1	x_1	w_1
z_2	y_2	x_2	w_2
z_3	y_3	x_3	w_3
z_4	y_4	x_4	w_4
z_5	y_5	x_5	0
z_6	y_6	x_6	0
z_7	y_7	0	0
z_8	0	0	0
z_9	0	0	0
z_{10}	0	0	0
z_{11}	y_8	x_7	w_5
β	β	$\beta = 0$	$\beta = 0$

Table 3.1: Equivalent coordinates of models

tions of motion for the system are composed of eleven coupled second order differential equations. Arranging these equations in the indicial form of equation 1 with indices running from 1 to 11 and the terms sorted by indicial order these equations contain not only the equations of motion for the system described, model 3, but also those of model 2, model 1 and the basic 2D model. Thus by making $z_8 = z_9 = z_{10} = 0$ the equations for model 2 (paper 2) result, by making $z_7 = z_8 = z_9 = z_{10} = 0$ and parameter $\beta = 0$ model 1 (paper 1) results and by putting $z_5 = z_6 = z_7 = z_8 = z_9 = z_{10} = 0$ and parameter $\beta = 0$ the 2D model of paper 1 is produced. In this procedure it is important to note that in model 1 the introduction of the $\beta = 0$ condition requires the moment of inertia tensor to be transformed to take account of the fact that the ligamental axis in the equilibrium condition is in the \mathbf{n}_2 direction with the roll axis in the \mathbf{n}_1 direction.

To avoid confusion in working with and comparing models it has been found necessary to denote each model's coordinates by a different letter. In order to maintain the indicial ordering within each model for the sake of equation generation and general understanding the various model coordinates are related to each other as in table 3.1. The only slight difference in coordinate matching in this scheme is that w_5 as defined in the 2D model is an inertial coordinate whereas in the three dimensional models $z_{11}/y_8/x_7$ are relative coordinates

3.2.4 Kineto-static forces and impulses

An important issue which will arise in considering the dynamics of model 3 is the establishment of the internal or kineto-static forces within the fused incudo-malleal block which hold the block together as it moves in space. This and the related issues

of the conditions associated with the opening and closing of the incudo-malleal joint are in turn related to the physical and mathematical problems inherent in transiting from model 2 to model 3 and vice versa- the relaxing and imposition of constraints respectively.

Since the literature relating to such issues within a multibody environment is both sparse and largely inapplicable to present concerns, paper 4 is presented which provides the background for some of the methods invoked in paper 3. In keeping with the notion of exploiting subsets of equations within a larger set, paper 4 demonstrates how the kineto-static forces are themselves contained as sub-sets within the wider equations of motion and how these are related to impulse equations governing transitions between models.

Chapter 4

Data and computation

The previous chapter has dealt with a number of issues that relate to the theoretical and symbolic nature of the equations of motion, equations (3.1). This chapter surveys the methods used to analyse the available parametric data and implement the numerical routines.

4.1 Derivation of parameters

In general it may be said the numerical parameters fall into two distinct groups; those which appear on the left hand side of the equations and are concerned with the kinematical description of the system, and those that appear on the right hand side concerned with the material aspects of the applied forces. Both the left and right sides of the equations depend upon the basic geometry of the bodies.

4.1.1 Geometry and inertial characteristics

Figure 3.3 is the redrawing of a more detailed set of scale drawings of a fused incudo-malleal block and it accompanying stapes, made by Weistenhofer & Hudde (1999). The original data Weistenhofer & Hudde data was derived by digitising eight angled profiles of the two bones and processing them by means of AUTOCAD to produce drawings, calculate the centres of masses, principal moments of inertia and the directions of principal axes.

This basic data was processed in three ways, the first being to generate basic geometrical information sufficient to allow decisions to be taken as to acceptable levels of model idealization. The second to provide the lengths and angles defined by the idealisations and the third to transform the principal moments of inertia of both bodies into the frames of reference used in models 1 and 2. The issue of the separation of the malleus and incus and the generation of their parameters as they affect model 3 is discussed below.

To accomplish these aims the basic drawings were digitised and scaled up to various scales to suit the circumstances. The three separate views of the incudo-malleal block where brought together and projected onto each other to ensure spatial and angular compatibility between the bodies and their individual reference frame projections, the process requiring only minor angular adjustments to be accomplish. The same technique was applied to the stapes and once completed both bodies were mated (as in figure 3.3) and their compatibility checked. These operations were undertaken using COREL 10 and the various measurement, scaling and orientation tools available in that program.

Once completed the three dimensional coordinates of the main points A_1, A_2 etc were measured and plotted independently to gauge the level of idealization required. The principal decision taken was to retain the angular orientation, β , of the ligamental axis in the $\mathbf{n}_1 \wedge \mathbf{n}_2$ plane but to reduce the angular orientation in the $\mathbf{n}_2 \wedge \mathbf{n}_3$ plane to zero to limit the amount of cross coupling. Using these basic decisions the remaining lengths defined by the framework in figure 3.3 were measured and then adjusted to ensure compatibility with the idealizations. Given the known angular orientation of the two bodies and their body fixed axes as described in chapter 3, the moments and products of inertia were calculated for the appropriate directions using the principal axis data converted to the body frames by the application of appropriate tensor transformations. The results of these length and inertial calculations are to be found in table 1, paper 2.

To convert the measurements of model 2 to those of model 1, whose essential geometric difference lies in the simplification introduced by making $\beta=0$, the ligamental axis's horizontal projection on to \mathbf{n}_2 was used. The result of this was to shorten the overall length of the chain and to re-orientate the body frame so that it lies parallel to \mathcal{N} in the equilibrium position. This in turn required recalculation of the moments and products of inertia whose results are given in table 5 paper 1.

Since the detailed length/geometrical data contained in Weistenhofer & Hudde (1999), treat the incus and malleous as a single rigid block it was necessary to disaggregate this data into its two constituent parts. To accomplish this recourse was made to Beer et al (1999) where mass and principal momental data for separate malleous and incus are available but with no specifically related length data provided. In comparing the two data sets the sum of the masses of malleus and incus as given by Beer et al (1999) is 52.6mg whilst that contained in Weistenhofer et al (1999) and used in models 1 and 2 is 52.8mg. Although these measurement only refer to a single parameter it was felt that they were sufficiently close as to warrant incorporating the incus data contained in Beer into the far more detailed data of Weistenhofer.

Although no other geometric data or scale other than mass and principal momental data is available in Beer, the drawing accompanying the data has attached to the incus at the incudo-stapedial joint, a right angled triad whose orientation

appears to be the same as the inertial Newtonian set $\mathcal N$ used in models 1 & 2, which given the principal axis orientation and symmetry of the stapes footplate may be considered as a naturally occuring orientated frame. Further, since the centre of mass of the combined incudo-malleal block lies on the anterior-posterior ligamental axis it was assumed that the incus's centre of mass would also lie on this line and as the Beer data gave the mass of the incus as $m_B=27.6mg$ and Weistenhofer's total mass was $m_A+m_B=52.8$, the mass of the malleus was taken to be $m_A=25.2$. Thus by using the above assumptions and transforming Beer's principal momental data into frame $\mathcal B$, the moment of interia characteristics of the malleus were derived by means of the deconstruction of the Weistenhofer data.

4.1.2 Material parameters and calculation of applied forces

Paper 1 discusses in reasonable detail the method of transforming the various parameters forming the Kringlebotn model from electroacoustic units to mg/mm/ms. After considerable testing these latter units were found to provide the most effective numerical measure in terms of understanding and relative size and were adopted as standard for all the mechanical models.

The transformations relating the conversion of acoustic/electrical units such as acoustic Ω , into the mg/mm/ms set require the use of a set of conversion factors which in turn depend upon the electrical 'transformer' constants of the circuit denoted by Kringlebotn as ' k_1, k_2, k_3 '; as shown in paper 1 these constants represent the basic geometry of the ear. The linear and rotational spring and damping constants for the posterior and anterior ligaments were derived by taking the Young and Poisson moduli listed in Koike & Wada(2002) and Ferris & Prendergast(2000), and by using the ligamental geometric data provided by Wever & Lawrence(1954), converting these values to the spring constant k's and damping factor c's listed.

Once the material parameters were derived they were used to construct the potential and Rayleigh functions for the total system from which the generalised forces were calculated by means of the appropriate differentiation. Since the potential and Rayleigh functions require the geometry of the system for their specification in addition to the constants, the resulting generalised forces derived from these functions are different for each of the three models.

The derivation of the nonlinear incudo-malleal joint characteristics discussed in paper 3 and the parameters upon which they are constructed uses data contained in Cancura (1980). The Cancura data set contains a series of horizontal linear deflection measurements of two points, one on the incus and the other on the malleus to which the same value of force is applied acting in the same horizontal direction. Other data regarding experimental set-up is missing beyond the information that each test specimen consisted of an intact middle ear system apart from the eardrum which was decoupled from the malleous. From the diagrammatic information provided it is assumed the point of application of the force applied to the incus is the

lenticular process with the force applied to the malleus lying in the same horizontal plane. In terms of model 3 this is taken to mean that \mathbf{F}_{inc} , the force on the incus is given by $\mathbf{F}_{inc} = |F| \mathbf{n}_1$ and its point of application is given by \mathbf{r}_{0B4} , similarly the malleous force is given by $\mathbf{F}_{mall} = |F| \mathbf{n}_1$ and its point of application by \mathbf{r}_{0A6} . The data lists four values of increases of \mathbf{r}_{0B4} and \mathbf{r}_{0A6} against four values of |F|. For the present purposes only the first two data points are used, that is the minimum force the joint can bear just prior to rupture, followed by the first measured deflection of the joint.

In considering the application of model 3 to this data set, model 3's coordinates have to be reduced by the removal of z_1, z_2 and z_3 to mirror the removal of the tympanic membrane so that model's coordinate set matching the data set is defined by the column vector $\{z\} = [z_4, z_5, z_6, z_7, z_8, z_9, z_{10}, z_{11}]^T$ with the further condition that prior to rupture $z_8 = z_9 = z_{10} = 0$ so that this prior-to-rupture condition state is given by the state set [1, 1, 1, 1, 1, 0, 0, 0, 1] as described in paper 3. On this basis the static nature of the data reduces all inertial and velocity terms in the equation of motion to zero leaving only stiffness and applied forces such that after manipulation $\{z^o\} = (K^o)^{-1} \{F^o\}$. In this expression K^o is the 6×6 matrix of stiffness coefficients related to z_4, z_5, z_6, z_7, z_8 and z_{11} , whilst $\{F^o\}$ is the column vector of applied forces generated by the application of \mathbf{F}^o_{inc} and \mathbf{F}^o_{mall} undergoing virtual displacements $\delta \mathbf{r}_{0B4}$ and $\delta \mathbf{r}_{0A6}$ respectively. The static deflection of the system $\{z^o\}$ under these loads can then be used to calculate the reaction torque M_{z_9} associated with this rupture condition, that is $M_{z_9} = M_o$.

To calculate the spring constant of the joint under the opening of the coordinate z_9 the state of the model is increased to [1,1,1,1,0,1,0,1] such that the active components are now $z_4, z_5, z_6, z_7, z_8, z_9, z_{11}$ and the second static position is defined by $\{z^1\}$ such that $\{z^1\} = (K^1)^{-1} \{F^1\}$. Here however K^1 is the 7×7 stiffness matrix related to the system's seven coordinates but with the known stiffness coefficient k_{99} augumented by κ such that $k_{99}^1 = k_{99} + \kappa$, where κ is the unknown linear coefficient of the joint. $\{F^1\}$ is derived in a similar fashion to $\{F^o\}$ using the given applied forces and their virtual displacements and in addition, for the F_9^1 component, the known rupture force $-sign(z9)M_o$ is added. Since from the data z_9^1 is known, an interative procedure can be implemented treating κ as the variable whose final value is determined when the $z_9 = z_9^1$.

4.2 Programing considerations

In general programing considerations can be broken down into three distinct types, the first is concerned with the generation of the equations of motion using *Sophia* together with the symbolic algebraic package Maple. The second is the solution of these equations using Matlab and the third is the generation of the graphical interpretations of derived quanties using Matlab. In what follows the latter will not be discussed further given their 'secondary' nature except to note that in pure

progaming terms the amount of programing in certain cases proved to be considerable. All calculations were carried out on an IBM $2656E\ 2G$ Think Pad machine with Intel Pentium(R) III, $1000\ processing$.

4.2.1 Sophia

Little need be said concerning the actual generation of the equations of motion using Sophia, the techniques being discussed in detail in Lesser(1995). The principal issue in using such a tool resides in checking the results due to the ease of creating computer-aided mistakes which are easily lost sight of in the mass of code. These mistakes can occur from failures in the actual symbolic manipulation, but more usually in the initial construction of basic data structures, such as frame of reference transformations and position vectors involving a number of different frames. Once these quantities have been established and confirmed, operations relating to them, such as their differentiation and amalgamation into derived quantities is a relatively straightforward matter, albeit one that requires considerable care and checking.

The equations of motion themselves were generated by Sophia using the scheme laid out in paper 1 to produce reactionless equations. Although the overall equations of motion were derived for model 3 with the other models being subsequently generated by equating the relevant coordinates to zero, it was felt necessary to guard against the type of coding errors discussed above. This was accomplished by independently constructing equations of motion (including frames and position vectors) for all the models concerned using their appropriate coordinate designations and comparing the result with that produced by the overall model. Similar checks were carried out for the potential and Rayleigh functions for each model.

Since the equations of motion were generated under the assumption that their degree of linearity/nonlinearity was a matter of investigation, all quantities were maintained in their full form for as long as possible with expansions of trigonometrical functions being performed to the third degree as late as possible in the process. As a final check, once the linearity of the equations had been confirmed all equations were rederived, using Sophia, by means of constructing system kinetic energies and applying the Lagrangian formulation.

4.2.2 The solution of equations

Since many of the solutions required were of steady state linear form with frequencies, amplitudes and phases being dependent upon the forcing frequency, it is a relatively straightforward matter to develop solution methods for these cases. The appropriate stiffness and viscous matrices were used to generate the necessary amplitude and phase quantities for given range of forcing frequency and input pressure, using Matlab with Maple as an independent check. To investigate the transient properties of the linear systems the differential equations were solved di-

rectly using the Matlab ODE 45 equation solver, Laplace transformations being found inadequate to deal with the degree of the equations involved. All Matlab calculations were carried out to absolute and relative errors of 10^{-9} , this being found to be most suitable.

In dealing with the nonlinear models, model 3 in paper 3 and the triple pendulum example of paper 4, extensive use was made of the binary, system state set, described in detail in paper 4 and mentioned above. This allowed the basic equation set to be utilised to enable movement between different configurations, calculating not only the appropriate coordinates and velocities but also the constraint forces involved. The method used to detect the presence of transitions conditions was the Matlab event function linked to a decision making procedure utilising the state set, the arrangement proved very effective, particularly in view of the complexity of the rupture conditions.

4.3 Numerical model equations

This section brings together the numerical versions of the various equations of motion examined by this thesis. In what follows the equations are expressed in the general form:

$$M_i = F_i$$

where M_i is the inertial term composed of the product of the generalised masses and their respective accelerations and F_i is the corresponding generalised force for coordinate i. For the sake of brevity and in conformity with the conclusions, the numerical values of the Christofell terms are not presented.

4.3.1 2D model

To render the terms below compatible with the theoretical discussion in the rest of the thesis the relationships listed in table 3.1 are employed. Thus the coordinates are related to each other by means of the expressions, $q1 = w_1$, $q2 = w_2$, $q3 = w_3$, $q4 = w_4$ and $q11 = w_5$, the velocities by $u1 = \dot{w}_1 \cdots u11 = \dot{w}_5$ and the accelerations by $u1t = \ddot{w}_1 \cdots u11t = \ddot{w}_5$.

Generalised inertias

$$Mq1 = 2.700u1t$$

$$Mq2 = 0.3600u2t$$

$$Mq3 = 23.76u3t$$

$$Mq4 = 142.30u4t + 23.80u11t$$

$$Mq11 = 23.80u4t + 28.00u11t$$

Generalised forces

$$Fq1 = -(276.9q3 - 900.0q2 - 947.4q4 + 2124.3q1 + 86.400u1 - 43.20u3 - 43.20u4)$$

$$Fq2 = -(900.0q1 + 992.31q2 + 21.60u2)$$

$$Fq3 := -(1476.9q3 - 276.9q1 - 43.20u1 + 50.400u3)$$

$$Fq4 = -(-1560.0q11 - 947.4q1 + 21474q4 - 43.20u1 - 2808.0u11 + 2210.4u4)$$

$$Fq11 = -(-1560.0q4 + 3114.4q11 - 2808.0u4 + 3851.2u11)$$

4.3.2 Model 1

The coordinates in this model are related to each other by the expressions, $q1 = x_1$, $q2 = x_2$, $q3 = x_3$, $q4 = x_4$, $q5 = x_5$, $q6 = x_6$ and $q11 = x_7$, the velocities by $u1 = \dot{x}_1 \cdots u11 = \dot{x}_7$ and the accelerations by $u1t = \ddot{x}_1 \cdots u11t = \ddot{x}_7$.

Generalised inertias

$$Mq1 := 2.700u1t$$

 $Mq2 := .3600u2t$
 $Mq3 := 23.76u3t$

Mq4 := 75.70u4t + 22.90u11t - 72.83u5t + 270.5u6t

$$Mq5 := -72.83u4t + 548.0u5t - 41.68u11t - 182.3u6t$$

$$Mq6 := 270.5u4t - 182.3u5t + 16.49u11t + 1743.u6t$$

$$Mq11 := 22.90u4t - 41.68u5t + 16.49u6t + 22.90u11t$$

Generalised forces

$$Fq1 = -(-276.9q3 - 900.0q2 + 2124.q1 - 947.4q4 + 86.40u1 - 43.20u3 - 43.20u4)$$

$$Fq2 = -(992.3q2 - 900.0q1 + 86.40u1 - 43.20u3 - 43.20u4)$$

$$Fq3 = -(1477.q3 - 276.9q1 - 43.20u1 + 50.40u3)$$

$$Fq4 = -(-947.4q1 + 1836.q4 - 1618.q5 + 640.1q6 + 889.05q11$$
$$-43.20u1 + 214.7u4 - 299.0u5 + 118.3u6 + 164.3u11)$$

$$Fq5 = -(-1618.q4 + 8998.q5 - 1165.q6 - 1618.q11$$
$$-299.0u4 + 544.4u5 - 215.2u6 - 299.0u11)$$

$$Fq6 = -(640.1q4 - 1165.q5 + 464.8q6 + 640.1q11 + 118.3u4 - 215.2u5 + 85.17u6 + 118.3u11)$$

$$Fq11 = -(889.05q4 - 1618.q5 + 640.1q6 + 2549.q11 + 164.3u4 - 299.0u5 + 118.3u6 + 3151.u11)$$

4.3.3 Model 2

The coordinates in this model are related to each other by the expressions, $q1 = y_1$, $q2 = y_2$, $q3 = y_3$, $q4 = y_4$, $q5 = y_5$, $q6 = y_6$, $q7 = y_7$ and $q11 = y_8$, the velocities by $u1 = \dot{y}_1 \cdots u11 = \dot{y}_8$ and the accelerations by $u1t = \ddot{y}_1 \cdots u11t = \ddot{y}_8$.

Generalised inertias

$$Mq1 = 2.700u1t$$

$$Mq2 = 0.360u2t$$

$$Mq3 = 23.760u3t$$

$$Mq4 = 75.702u4t - 72.834u5t + 250.516u6t - 101.926u7t + 22.902u11t$$

$$Mq5 = -72.834u4t + 619.296u5t - 447.823u6t - 616.844u7t - 41.682u11t$$

$$Mq6 = 250.516u4t - 447.823u5t + 1685.710u6t - 207.134u7t + 15.274u11t$$

$$Mq7 = -101.926u4t - 616.844u5t - 207.134u6t + 1571.086u7t - 6.214u11t$$

$$Mq11 = 22.902u4t - 41.682u5t + 15.274u6t - 6.214u7t + 22.902u11t$$

Generalised forces

$$Fq1 = -(-276.923q3 - 900.000q2 + 2124.291q1 - 947.368q4 + 86.400u1 - 43.200u3 - 43.200u4)$$

$$Fq2 = -(992.308q2 - 900.000q1 + 21.600u2$$

$$Fq3 = -(1476.923q3 - 276.923q1 - 43.200u1 + 50.400u3)$$

$$Fq4 = -(-947.368q1 + 1962.782q4 - 762.961q5 + 586.887q6$$

$$-1966.973q7 + 880.007q11 - 43.200u1 + 108.457u6$$

$$-44.195u7 + 213.031u4 - 295.946u5 + 162.625u11)$$

$$Fq5 = -(-762.962q4 + 8109.209q5 - 1068.134q6$$

$$-10269.102q7 - 1601.613q11 - 197.392u6$$

$$+79.894u7 - 295.946u4 + 538.885u5 - 295.979u11)$$

$$Fq6 = -(586.887q4 - 1068.134q5 + 398.879q6$$

$$-159.250q7 + 586.887q11 + 72.331u6$$

$$-29.429u7 + 108.457u4 - 197.392u5 + 108.457u11)$$

$$Fq7 = -(-1966.973q4 - 10269.102q5 - 159.250q6 +22121.601q7 - 238.787q11 - 29.429u6 +12.834u7 - 44.195u4 + 79.894u5 - 44.127u11)$$

$$Fq11 = -(880.007q4 - 1601.613q5 + 586.887q6$$

$$-238.787q7 + 2522.687q11 + 108.457u6$$

$$-44.127u7 + 3119.449u11 + 162.625u4 - 295.979u5)$$

4.3.4 Model 3

The coordinates in this model are related to each other by the expressions, $q1=z_1$, $q2=z_2$, $q3=z_3$, $q4=z_4$, $q5=z_5$, $q6=z_6$, $q7=z_7$, $q8=z_8$, $q9=z_9$, $q10=z_{10}$ and $q11=z_{11}$, the velocities by $u1=\dot{z}_1\cdots u11=\dot{z}_{11}$ and the accelerations by $u1t=\ddot{z}_1\cdots u11t=\ddot{z}_{11}$.

Generalised inertias

$$Mq1 = 2.700u1t$$

$$Mq2 = 0.360u2t$$

$$Mq3 = 23.760u3t$$

$$Mq4 = 75.702u4t - 72.834u5t + 250.516u6t - 101.926u7t$$

 $-47.214u8t - 86.763u9t + 35.301u10t + 22.902u11t$

$$Mq5 = -72.834u4t + 619.296u5t - 447.823u6t - 616.844u7t$$

 $+130.035u8t + 158.941u9t - 51.620u10t - 41.682u11t$

$$Mq6 = 250.516u4t - 447.823u5t + 1685.710u6t - 207.134u7t$$

 $-121.912u8t + 17.489u9t - 34.336u10t + 15.274u11t$

$$Mq7 = -101.926u4t - 616.844u5t - 207.134u6t + 1571.086u7t + 7.330u8t + 16.444u9t + 106.130u10t - 6.214u11t$$

$$Mq8 = -47.214u4t + 130.035u5t - 121.912u6t + 7.330u7t + 79.383u8t + 103.410u9t - 41.458u10t - 28.169u11t$$

$$Mq9 = -86.763u4t + 158.941u5t + 17.489u6t + 16.444u7t + 103.410u8t + 406.895u9t - 133.824u10t - 86.763u11t$$

$$Mq10 = 35.3007u4t - 51.620u5t - 34.336u6t + 106.130u7t -41.458u8t - 133.824u9t + 152.816u10t + 35.301u11t$$

$$Mq11 = 22.902u4t - 41.682u5t + 15.274u6t - 6.214u7t$$

 $-28.169u8t - 86.763u9t + 35.301u10t + 22.902u11t$

Generalised forces

$$Fq1 = -(-276.923q3 - 900.000q2 + 2124.291q1 - 947.368q4 + 86.400u1 - 43.200u3 - 43.200u4)$$

$$Fq2 = -(992.308q2 - 900.000q1 + 21.600u2$$

$$Fq3 = -(1476.923q3 - 276.923q1 - 43.200u1 + 50.400u3)$$

$$Fq4 = -(-947.368q1 + 1962.782q4 - 762.961q5 + 586.887q6 - 1966.973q7 - 1082.409q8 - 3333.843q9 + 1356.445q10 + 880.007q11 - 43.200u1 + 108.457u6 - 44.195u7 - 200.030u8 - 616.096u9 + 250.667u10 + 213.031u4 - 295.946u5 + 162.625u11)$$

$$Fq5 = -(-762.962q4 + 8109.209q5 - 1068.134q6$$

$$-10269.102q7 + 1969.984q8 + 6067.594q9 - 2468.730q10$$

$$-1601.613q11 - 197.392u6 + 79.894u7 + 364.055u8$$

$$+1121.297u9 - 456.216u10 - 295.946u4 + 538.885u5 - 295.979u11)$$

$$Fq6 = -(586.887q4 - 1068.134q5 + 398.879q6$$

$$-159.250q7 - 721.871q8 - 2219.639q9 + 904.629q10$$

$$+586.887q11 + 72.331u6 - 29.429u7 - 133.402u8$$

$$-410.882u9 + 167.173u10 + 108.457u4 - 197.392u5 + 108.457u11)$$

$$Fq7 = -(-1966.973q4 - 10269.102q5 - 159.250q6 +22121.601q7 + 293.708q8 + 904.629q9 - 368.067q10 -238.787q11 - 29.429u6 + 12.834u7 + 54.277u8 + 167.173u9 -68.017u10 - 44.195u4 + 79.894u5 - 44.127u11)$$

$$Fq8 = -(-1082.409q4 + 1969.984q5 - 721.871q6 \\ +293.708q7 + 1331.363q8 + sign(q8)(0.72) + 1495.00q8 + 4100.627q9 \\ -1668.427q10 - 1082.409q11 - 133.402u6 + 54.277u7 \\ +246.037u8 + 757.799u9 - 308.322u10 - 200.030u4 \\ +364.055u5 - 200.030u11)$$

$$Fq9 = -(-3333.843q4 + 6067.594q5 - 2219.639q6 \\ +904.629q7 + 4100.627q8 + 12633.759q9 + sign(q9) (0.72) + 1495.00q9 \\ -5138.793q10 - 3333.843q11 - 410.882u6 + 167.173u7 \\ +757.800u8 + 2334.039u9 - 949.637u10 - 616.096u4 \\ +1121.297u5 - 616.096u11)$$

$$Fq10 = -(1356.445q4 - 2468.730q5 + 904.629q6$$

$$-368.067q7 - 1668.427q8 - 5138.793q9$$

$$+2090.828q10 + sign(q10) (0.72) + 1495.00q10 + 1356.445q11 + 167.173u6$$

$$-68.017u7 - 308.322u8 - 949.637u9 + 386.374u10$$

$$+250.667u4 - 456.216u5 + 250.667u11)$$

$$Fq11 = -(880.007q4 - 1601.613q5 + 586.887q6$$

$$-238.787q7 - 1082.409q8 - 3333.843q9$$

$$+1356.445q10 + 2522.687q11 + 108.457u6$$

$$-44.127u7 - 200.030u8 - 616.096u9 + 250.667u10$$

$$+3119.449u11 + 162.625u4 - 295.979u5)$$

Chapter 5

Conclusions and outlook

Although each paper presents a list of conclusions relevant to it's particular theme, this chapter brings them together to form a summarized and generalised version for which claims of originality are made. Based upon these overall conclusions a number of suggestions are made for further work in areas where it is thought viable results can obtained for a relatively modest investment of resources.

5.1 Conclusions

Linearity vs nonlinearity of ossicular motion- papers 1 and 2

It has been demonstrated that under the accepted view of the incudo-malleal block as being a singular fused entity, the three dimensional motion of the ossicular chain is linear in nature. This conclusion is tested and holds for an increase in complexity brought about by increasing the degree asymmetry of the block's geometry.

The reason for this linearity, is that the geometrical configuration of the block is such as to ensure the numerical values of displacements, velocities and accelerations are of the same small order of numerical magnitude. When these quantities appear in multiplicative combination, as in variable mass terms, their effects become negligible. This means that only constant generalized mass terms remain in the accelerative portion of the equations of motion and since the applied potential and damping forces are dependent upon the provision of linear data, linear equations result.

Resonance characteristics- papers 1 and 2

Using models 1 and 2, it is shown that the incudo-malleal block has three resonant frequencies. The lowest is resonance in yaw which is of such low value, 11 Hz, that it may be considered outside the frequency range covered by this investigation. The second is a resonance in roll at a frequency of approximately 300Hz. The

strongest resonance, virtually unaffected by the increase in complexity of model 2 over model 1, is the resonance in pitch found at 600Hz. As far as is known these resonances have not been described before and underline the low frequency nature of the chain's characteristics.

Analysis of the chain's resonant frequencies for changes in the scale of the lineal dimensions of the incudo-malleal block yield proportionate changes, confirming in general the robust nature of the device.

Axodal characteristics- paper 2

As opposed to the standard fixed axis hypothesis describing ossicular motion it is demonstrated that the motion traced out by the velocity screws (the axodes), of both the incudo-malleal block and the stapes are not fixed in space, even approximately. The dimensions of both reference curves, (ellipses), traced out by the intersection of the two axodes and their reference planes are of the same order as the dimensions of the malleus and stapes respectively. The form of the axode in both cases is shown to be a möbius one-sided surface whose characteristics are due to the change in direction of the respective velocity screws traversing their respective axodes twice during an input cycle.

Impulse axis of rotation- paper 2

The possibility that a fixed axis model might be an acceptable description for a static or near static equilibrium pose is investigated for the case where an impulse is applied to the incudo-malleal block. It is found that although not coinciding with the ligamental axis such an impulse screw is located approximately in a horizontal plane drawn through the axis and might be sufficient to account for the claim of fixity.

On the basis of this conclusion it is judged the fixed axis hypothesis does not provide a satisfactory model for describing the motion of the ossicular chain during steady state forced motion but might be approximately valid for near static conditions.

Force and velocity screws-paper 2

Using the dual of the velocity screw, the force screw, the power relationships between these two entities for both the incudo-malleal block and the stapes are analysed and then visualized to illustrate the screw relationships involved.

Nonlinear behaviour and the incudo-malleal joint- paper 3

In considering the proposition that the incudo-malleal block is not a fused single body but two separate bodies (the malleus and the incus), capable of movement relative to each other via the incudo-malleal joint, it is demonstrated that on the evidence available the motion generated is of nonlinear form. This form becomes apparent at high, but physiologically acceptable, driving pressures above SPL 104.

Mode of incudo-malleal joint operation- paper 3

Consideration of the operation of the incudo- malleal joint shows it to have preferred planes of action, the principal plane being the pitching plane. Although it is necessary for the driving pressure to be above SPL 104 for the joint to be activated this is not a sufficient condition to guarantee a functioning joint since it is also shown there is a frequency dependency up to SPL 122, beyond which the joint will operate regardless of input frequency.

It is demonstrated that the basic mechanism activating the joint's functioning are the internal kineto-static (rupture) forces generated by the motion.

Frequency dependency of joint operation- paper 3

It is shown that the joint is more likely to be activated at low rather than high frequencies due to the high displacements and associated high accelerations experienced under such conditions. Such conditions are always to be found in transitional as well as steady state operating conditions, the former being experienced by the imposition of impulse loading.

Effect of joint operation- paper 3

It is demonstrated that the joint, when it is operating, acts as an efficient energy dissipator in its preferred plane of pitch operation. The implication of this is that since the second preferred plane of operation is the roll plane, the joint has the ability to have a graded dissipator response to disturbances with subsequent alterations in the trajectory of the chain's constituents.

The imposition and removal of constraints- paper 4

The dynamical requirements for the operation of the incudo-malleal joint depend upon the ability to be able to decide when and when-not-to impose the joint's geometrical constraints in the equations of motion. This dynamical issue is considered separately in paper 4 although its results and methods are applied in paper 3.

As part of the overall notion of equation embedding it is shown how constraint forces are held within the higher degree of freedom system equations and how an ordered set of binary numbers can be used to act as configuration specifiers. Such a system allows the highest degree of freedom equations to be manipulated to reach all possible smaller degree of freedom configurations.

Using Lagrangian concepts of generalized impulse it is also shown how the transition between constraints and the decision at to their imposition or not can be

decided. The results are generalised to include the imposition of constraints using redundant coordinates.

5.2 Future work

In considering the possibility of future work in the light of the above conclusions a series of suggestions are listed below under the headings of 'Experimental', 'Theoretical' and 'Prosthesis'. Inevitably most of the items in any one category also have ramifications for the others so in this sense the suggestions should be viewed as being inclusive in scope.

In compiling these suggestions, a number of exploratory investigations have been undertaken to gain a measure as to what might be possible and to test the validity of some underlying ideas. These calculations have centred in the main upon the roles of the tensor and stapedial muscles in both their singular and joint functioning, modelled as massless directed forces, adjoined to model 3.

In particular the effects of the two muscles upon the static pose of the chain and the probable dynamics of the incudo-malleal joint working under such conditions were briefly examined. The principal reason for undertaking these informal calculations was to gauge the practicality of constructing a model of the acoustic reflex, a phenomenon that as far as is known only planar acoustic models have been used to address to date. Since the informal calculations ranged in rigour and application from back-of- the-envelope estimates to a limited number of specific simulations, they are not put forward as firm conclusions or evidence but it is felt their fact suggests very strongly that the methods and ideas developed in this thesis have considerable potential for further development.

5.2.1 Experimental

Construct an 'atlas' of the ossicular chain and the middle ear cavity

The type of data available as to the actual geometry and configuration of the middle ear is very patchy and some of it is very old. Although data is known from a variety of sources, most of it is unsystematic and only in the rarest of cases is it given with respect to some defined reference triad. To meet this basic geometrical need it is suggested an atlas of the middle ear be constructed.

This atlas or mapping should include in addition to the ossicular chain and its components, all the associated suspensory ligaments and muscles together with their dimensions and anchoring points. The production of such an atlas, which given modern imaging technology should be a relatively straightforward procedure, would provide a set of coherent consecutive data sufficient to formulate something like a standard middle ear for reference and modelling.

Material Characteristics

There is a need for the proper evaluation and publication of the linear and nonlinear characteristics (including damping), of the material found in the middle ear particularly that relating to the suspensory and annular ligaments in both their axial and torsional modes. The ideal situation would be to use the material from which the atlas is derived so that it would be possible to relate the geometry directly to the material.

Muscle charcteristics

Informal calculations suggest that the size of forces reported to be generated by the tensor and stapedius muscles, Lutman(1975), are far too high for what the ossicular chain could withstand unless nonlinear effects are present. Given the importance of the stapedius muscle (and perhaps the tensor muscle as well) in the action of the acoustic reflex an evaluation of both muscles (preferably those mapped using the information in the atlas), would make a major contribution to unraveling this important physiological issue.

Incudo-malleal joint characteristics

Although the pioneering work of Hüttenbrink (1988) concerning the physiology and mechanics of the incudo-malleal joint under static pressure is recognised, a geometrical mapping of the joint's external and internal geometry together with an evaluation of the material characteristics of its encapsulment would greatly add to its understanding. Of particular interest is the determination of the joint's opening and directional properties. Such characteristics should also include three dimensional measurement of its torque/displacement characteristics.

The incudo-stapedial joint

Although the incudo-stapedial joint has not featured in this work it is felt the situation regarding its material and measured charcteristics is similar to that of the incudo-malleal joint. Basic measurements as to the physiology and kinematical scope of the incudo-stapedial joint appear to be lacking and deserve attention. Hüttenbrink (1988) suggests that this joint's function is to move in a plane normal to the prevailing piston motion of the stapes footplate, thereby acting as a force dissipator, this may well suggest some sort of nonlinear behaviour.

Static force/displacement experiments

Mechanical/kinematic knowledge as to the overall workings of the middle ear, given the geometrical atlas referred to above, could relatively easily be enhanced by applying a series of known static forces to the chain and measuring the overall deflections and relative movement of the individual members. This is particularly the case for the application of force in the direction of the stapes and tensor muscles, both independently and concurrently.

5.2.2 Theoretical

The acoustic reflex

Much modelling activity of the middle ear has been aimed at understanding the ear's acoustic reflex, the involuntary response of the ear to loud noises. As far as is known all this activity has been undertaken using acoustic models where the action of the reflex is modelled in the steady state only by increasing the numerical stiffness (inverse capacitance) of the incudo-stapedial joint. None of the known models investigate the process as a physical phenomenon working in three dimensional space and the treatment of the control and transient nature of such events is very limited.

With relatively modest effort the models contained in this thesis can be easily adapted to incorporate such a mechanism and by the incorporation of a feedback loop/loops the essentials of the control problem can begin to be addressed.

The role of the tensor and stapedius muscles

Related to the acoustic reflex but separate from it are the roles of the tensor and stapedius muscles. Although the stapedius muscle is generally credited with the reflex function the role of the tensor muscle is much less well defined. Excluding the effect of the reflex action the informal calculations suggest that both muscles have a considerable effect upon the static pose of the chain. Indeed, given the 'lever' arms involved, and excluding the appearance of nonlinear material characteristics, it appears possible that large deflection angles of pose can be generated by means of small muscle forces applied both individually and in concert. It seems possible that the small angle assumptions of geometrical linearity can be relatively easily violated by means of the application of these muscles.

The informal calculations also suggest that the stapedius muscle, but not the tensor, has the ability to open the incudo-malleal joint, in addition to the kineto-static forces discussed here. This raises the prospect that the acoustic reflex could also involve such an effect as well. As far as is known no such interaction has been proposed before.

Modelling of the incudo-malleal and incudo-stapedial joints as kinematical entities

It will be clear from this thesis that apart from basic physiological descriptions of the middle ear's two joints, no work has been located which discusses the kinematical aspects of their functioning. Given the amount of kinematical research devoted to understanding the movement of the more accessible and visible joints of the human body, it is felt this is particularly fruitful and untouched area suitable for kinematical investigation. It is also an area suitable for investigation via the calculus of screws, particularly in the area of visualization.

Chaotic motions

It is well known that chaotic motion, in the sense that small changes in the initial conditions of a set of equations can lead to large differences in final system configurations, is frequently present in systems possessing discontinuities such as impacts. Such chaotic motion is also well attested to in systems involving jerk motion, Sprott(1997).

If it is accepted that the imposition and removal of constraints, as discussed in papers 3 and 4 and applied to the motion of the incudo-malleal joint, fall within these jerk and impulse categories, tentative calculations suggest that sensitivity to parameter change is possible which might in turn indicate the presence of chaotic motion under the right conditions. Consequently it is felt an examination of the functioning of the middle ear joint, perhaps using some measure of simplification, could well reveal chaotic motion. It would then be possible to examine its physical reality and allow its consequences to be assessed.

5.2.3 Prosthesis

The subject of prosthesis construction has not been touched upon apart from the introductory remarks. However in considering such an issue it is felt the type of mathematical models discussed here could be used with advantage to investigate the possibility of developing a prosthesis design technique. It is envisaged that it might be possible to engineer the material characteristics of a given device to take account of the three dimensional nature of the movement involved, including the joint, and thereby improve performance, something that is not done at present. This suggestion should be a relatively straightforward matter to investigate perhaps by utilizing an optimising technique such as a genetic algorithm.

References

WRIGHT T.(2001); The nonlinear dynamics of mechanical frogs and similar toys, Licentiate Thesis, SRN/KTH/MEK/TR–01/14–SE, Royal Institute of Technology, Stockholm.

KINSLER L.E., FREY A.R., COPPENS A.B., SANDERS J.V., (2000); $Fundamentals\ of\ acoustics$, 4th ed., Wiley

MØLLER A.R., (1970); The middle ear. In Foundations of Modern Auditory Theory, vol. 2, (J.V. Tobius, ed.), Academic Press.

NUMMELA S.,(1995); Scaling of the mammalian middle ear, $Hearing\ Research$, 85, p18-30.

YOST W.A. (2000); Fundamentals of Hearing, Academic Press.

GLASER R,(2001); Biophysics, Springer Verlag.

HERSH M.A., JOHNSON M.A., (2001), The hearing-impaired, deaf and deafblind, Springer.

KOIKE T., WADA H, (2002); Modeling of the human middle ear using the finite element method, *J. Acoust. Soc. Am.*, **111**, p1306-1317.

PASCAL J., BOURGEADE A., (1998); Linear and nonlinear model of the human middle ear, *J. Acoust. Soc. Am.*, **104**, p1509-1516.

HUDDE H., WEISTENHÖFER C., (1997); A three-dimensional circuit model of the middle ear, *Acustica*, **83**, p535-549.

ZWISLOCKI J., (1962); Analysis of the middle ear function. Part I: Input impedance, J. Acoust. Soc. Am., 34, p1514-1523.

RAVEN, F.H., (1968); Automatic Control Engineering, 2nd ed, Mcgraw-Hill

LUTMAN, M.E. & MARTIN, A.M.(1979); Development of an electroacoustic analogue model of the middle ear and acoustic reflex, *Journal of Sound and l Vibration*, 64, p133-157.

KARNOPP, D.C., MARGOLIS, D.L. & ROSENBERG R.C., (2000); $System\ Dynamics$, 3rd ed., Wiley.

SYNGE, J.L.,(1926); On the geometry of dyanamics, *Phil.Trans.Roy. Soc.*, series A, 226, p31-206.

BLOCK, A.M, BAILLIEUL J. CROUCH P. & MARSDEN J; (2000), Nonholonomic Mechanics and Control, Springer Verlag.

BALL, R., A., (1998, reprint of 1st ed. 1900); A Treatise on the Theory of Screws, Cambridge University Press.

BOTTEMA, O., & ROTH, B., (1990); Theoretical Kinematics, Dover.

PHILLIPS, J., (1990); Freedom in Machinery, vol. 2, Cambridge University Press.

WEISTENHÖFER C., HUDDE H., (1999); Determination of the shape and inertia properties of the human auditory system, *Audio. Neurootol*, 4, p192-196.

BEER H., BORNITZ M., HARDTKE H., SCHMIDT R., HOFMANN G., ZAHNERT T., HÜTTENBRINK K., (1999); Modelling of components of the human middle ear and simulation of their dynamic behaviour, *Audiol Neurootol*, 4,156-162.

KOIKE T., WADA H., (2002), Modeling of the human middle ear using the finite-element method, $J.Acoust.Soc\ Am$, 111, p1306-1317.

FERRIS P., PRENDERGAST P.J., (2000), Middle ear dynamics before and after ossicular replacement, *J.Biomechanics*, p581-590.

WEVER E.G. & LAWRENCE M., (1954), *Physiological Acoustics*, Princton University Press.

CANCURA W,.(1980); On the statics of malleus and incus and on the function of the malleus incus joint, *Acta Otolaryngol*, **89**, 342-344.

LESSER, M.,(1995); The Analysis of Complex Nonlinear Mechanical Systems, World Scientific.

LUTMAN, M.E., (1976); The protective action of the acoustic reflex, *Ph.D. thesis*. University of Southampton.

HÜTTENBRINK, K.B. (1988); The mechanics of the middle ear at static air pressures, *Acta Oto-laryngologica*, supplement 451, Stockholm.

SPROTT, J.C., (1997); Some simple chaotic jerk functions, Am.J.Phys , ${\bf 65}, p537-543.$